

Reply to anonymous Referee No.1: Multipoint Reconstruction of Wind Speeds

Christian Behnken, Matthias Wächter, and Joachim Peinke

Institute of Physics/ForWind, University of Oldenburg.

Correspondence: Peinke (peinke@uni-oldenburg.de)

Copyright statement. TEXT

NOTE: All figure and equation numbers refer to the original submitted manuscript and may differ from the ones in the revised version.

- 5 **Page 1, line 2: The authors introduce the abbreviation ‘cpdfs’, but inconsistently use ‘conditional pdf’ (e.g. Page 3, line 86) throughout the paper. This should be consistent.**

Changed in the revised manuscript.

- 10 **Page 2, line 28: Define what ‘short time scales’ means and how it relates to intermit- tency.**

We added following explanation to the revised manuscript:

“With short time scales we refer to time scales in the range of seconds to minutes. As it can be seen in (Boettcher et al., 2003). The effect of intermittency is most prominent at time scales < 1 s, but as the time scales increase, the pdfs broaden.”

- 15 **Page 2, line 35: How is the complexity of the wind energy conversion process con- nected to the desire of finding 3D velocity fields?**

To avoid misunderstanding we reformulated our sentence in the manuscript:

“The missing of the basic understanding, the impracticability of handling such huge data sets as well as the complexity of the wind energy conversion process leads often to the demand of simplified models for wind speed.”

- 20 in a new way:

“The impracticability of having all details of a turbulent wind field leads to the demand of the praxis to have access to simplified models for wind speed.”

Page 3, line 60: ‘1 min’ should read ‘1 minute long’.

25

Changed accordingly.

Page 3, line 60: Even though $U(t)$ is an obvious reference to a velocity, it should be defined in the text (especially as to see whether it is the mean of the full 3D velocity vector or of one component).

30

We added a definition in the revised manuscript: “With $U(t)$ we refer to the resulting wind speed from the horizontal components.”

Page 3, line 60ff: How much data was used?

35 We added the information in the manuscript: “The data were recorded at a sampling frequency of 1 Hz between calendar week 1 to 10 in 2007 with an ultrasonic anemometer, mounted at 80 m height, resulting in approximately $6 \cdot 10^6$ samples.”

Page 3, line 64f: It should be spelled out what these abbreviations are meant to abbreviate.

Changed accordingly.

40

Page 3, line 65f: Is this normalization justified? There could potentially a strong coupling between the mean and the standard deviation that erroneously gets averaged by this procedure. The authors should provide a plot of standard deviation vs mean for their dataset to build confidence in this grouping of blocks.

45 Indeed there is a significant coupling between mean wind speeds and fluctuations. Measuring the strength of the fluctuations by means of the standard deviation, we detect a quadratic scaling between both quantities (fig. 1). However we aim at modelling the quasi-stationary wind speed fluctuations $u^*(t)$, which are obtained by a blockwise normalization (of 1 min length) with respect to the mean and standard deviation of wind speeds $U(t)$. This way we decouple the fluctuations from the magnitude of the mean flow. As stated later on, a rescaling of the fluctuations is achieved when we transform the modelled fluctuations $u^*(t)$
50 back to real wind speeds U^* , by multiplying it with the standard deviation: $U^* = (\sigma_U \cdot u^*) + U$.

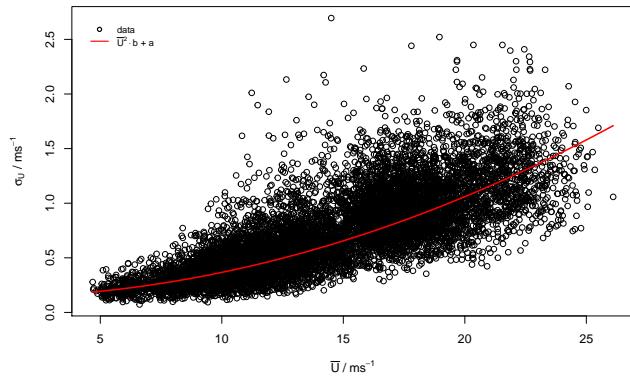


Figure 1. dependency of standard deviation σ_U on mean flow \bar{U}

Page 3, line 68: Explain how the wind speeds emerge from a turbulent cascade.

It is well known that the turbulent behavior of wind speed below 10 min becomes similar to the ideal homogeneous isotropic
 55 turbulence involving a turbulent cascades from large to small scales. The common arguments are that below 10 min the wind
 turbulence becomes three dimensional whereas for larger time scales the turbulence is more like a two dimensional turbulence
 with a cascade to larger scales. This transition between two and three dimensional turbulences with different directions of
 the cascade, in which the energy is transported, supports the idea of the similarity between three dimensional homogeneous
 isotropic turbulence and wind turbulence on smaller scales. A statistical analysis of wind data supporting this results are given
 60 in (Morales et al., 2012).

**Page 3, line 78: Taylors frozen flow hypothesis only holds if the fluctuations are small compared to the mean flow. Is
 this the case here? Provide numbers.**

As one can see from the provided histogram of the fractions of the fluctuations u^* and the mean flow \bar{U} (cf. fig. (2)), in most
 of the samples the fluctions are at least one magnitude smaller than the mean flow. In accordance we could add to our paper
 the comment that we use Taylors frozen flow hypothesis as an approximation, which might be improved in future.
 However our statement about Taylos frozen flow hypothesis was just supposed to be a general remark regarding the term 'multi-
 point' in the context of time series. As we are dealing with time series here, there is no check the validity Taylors hypothesis
 70 in our paper.

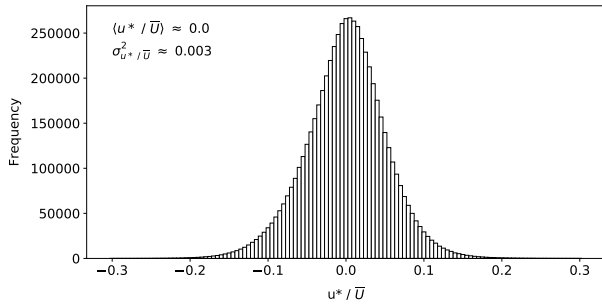


Figure 2. dependency of standard derivation σ_U on mean flow \bar{U}

Page 3, line 86: The abbreviation ‘lhs’ (and ‘rhs’) should be defined, even if it is commonly used.

Changed accordingly.

75 **Page 4: The derivation appears unwieldy (and is a reproduction of previous work) and might be better suited for supplemental materials.**

We removed this part of the method section accordingly and shifted it to the appendix.

80 **Page 4, line 102: The N. Reinke reference is missing a year.**

Changed accordingly.

Page 5, line 105: The citation style for Risken 1996 is different from other references.

85

Changed accordingly.

Page 5, line 109: The argument on the minus sign seems handwaving. Even though it is commonly repeated, a more rigorous, mathematical explanation would be desirable.

90

The minus (eq. (8)) is motivated by the fact that we consider the turbulent cascade going from large to small scales. With loss of generality a positive sign may be used (see (Peinke et al., 2019)).

Page 5, 110: Provide a reference for the Pawula theorem.

95

We added the reference in the revised manuscript (Risken 1996).

Page 5, line 111: Provide a plot in the manuscript to show that this approximation is valid for the data at hand.

100 We added a plot in the the revised manuscript: “As one can see in fig. (3), the fourth Kramery-Moyal coefficient is slightly larger than zero, but negligible compared to the magnitude of the diffusion function $D^{(2)}$ ”

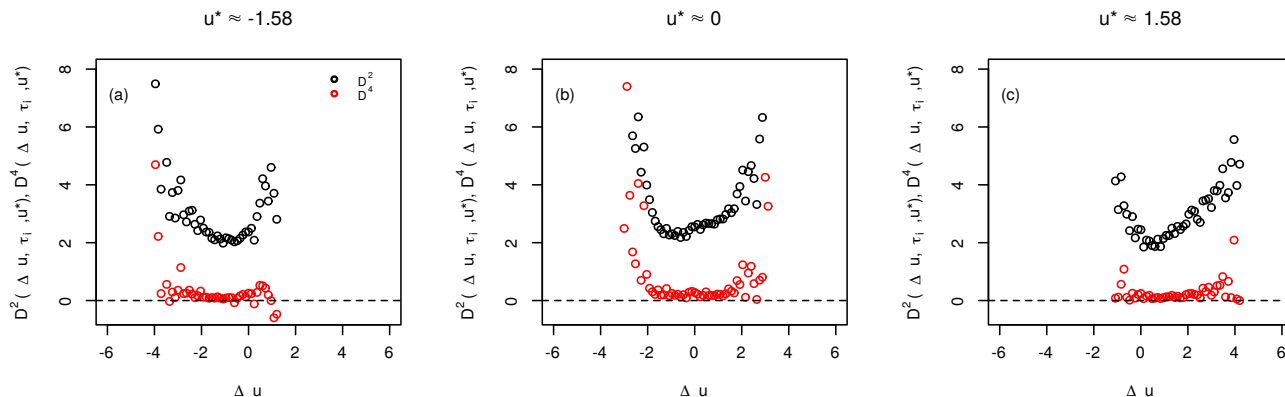


Figure 3. Exemplary estimations of the second and fourth Kramers-Moyal coefficient $D^{(2)}$ and $D^{(4)}$ for $\tau = 65$ s

Page 5, line 118: I disagree with the statement that ‘it can be easily seen’. Provide more details.

We added are more detailed explanation in the revised manuscript.

105

Page 6, line 139: The authors only check the validity of equation 15 for a single choice of the difference time tau = 1s. Given the potential of long-range correlations or eddies in the flow, this expression should be checked for several choices of tau.

110 The validity of equation 15 has been checked for a time scale separation $\Delta\tau_{EM} = 0.1$ s, being the Einstein-Markov length for this data set, and as well for $\Delta\tau > 0.1$ s, namely $\Delta\tau = 10 \cdot \Delta\tau_{EM} = 1.0$ s (see fig. 2) shown within our paper. As described in the beginning of the method section, the wind speeds $U(t)$ are transformed to quasi-stationary wind speed fluctuations $u(t)$, thus long-range correlations (longer than 1 min) will be eliminated by that procedure.

115 **Page 7, figure 1: The isoline heights are hard to read.**

Changed accordingly.

Page 7, line 156: Introduce abbreviations.

120

Added accordingly.

Page 8, line 160: What is d_{10} , etc?

125 The polynomial coefficients $d_{ij}(\tau_i, u^*)$ are themselves higher-order polynomial obtained from fitting the the third and second order polynomial coefficients over all considered τ_i and u^* . We explicitly obtained following polynomials (and added them to the appendix of the revised manuscript):

$$d_{10} = c_{0,d_{10}} \cdot \tau_i + c_{1,d_{10}} \cdot u^* \cdot \tau_i^{\tilde{c}_{1,d_{10}}} + c_{2,d_{10}} \cdot \tau_i^{\tilde{c}_{2,d_{10}}} \cdot u^{*2} + c_{3,d_{10}} \cdot u^{*3} \quad (1)$$

$$d_{11} = c_{0,d_{11}} \cdot \tau_i + c_{1,d_{11}} \cdot \tau_i^{\tilde{c}_{1,d_{11}}} + c_{2,d_{11}} \cdot \tau_i^{\tilde{c}_{2,d_{11}}} \cdot u^{*2} \quad (2)$$

130 $d_{13} = c_{0,d_{13}} \cdot \tau_i^{\tilde{c}_{0,d_{13}}} + c_{1,d_{13}} \cdot u^* \quad (3)$

$$\gamma_{D^{(1)}} = c_{1,\gamma_{D^{(1)}}} \cdot \tau_i^{\tilde{c}_{1,\gamma_{D^{(1)}}}} \cdot u^* \quad (4)$$

with $c_{0,d_{10}} = -0.006$, $c_{1,d_{10}} = -0.888$, $\tilde{c}_{1,d_{10}} = 0.098$, $c_{2,d_{10}} = 0.137$, $\tilde{c}_{2,d_{10}} = 0.019$, $c_{3,d_{10}} = -10.566$, $c_{0,d_{11}} = -1.656$, $c_{1,d_{11}} = -0.018$, $\tilde{c}_{1,d_{11}} = -8.853e - 05$, $c_{2,d_{11}} = -0.268$, $\tilde{c}_{2,d_{11}} = 1.671$, $c_{0,d_{13}} = -0.005$, $\tilde{c}_{0,d_{13}} = 0.012$, $c_{1,d_{13}} = 1.023$, $c_{1,\gamma_{D^{(1)}}} = 0.341$, $\tilde{c}_{1,\gamma_{D^{(1)}}} = 0.247$.

135

And for the diffusion function:

$$d_{20} = c_{0,d_{20}} \cdot \tau_i^{\tilde{c}_{0,d_{20}}} + c_{1,d_{20}} \cdot \tau_i^{\tilde{c}_{1,d_{20}}} \cdot u^* + c_{2,d_{20}} \cdot \tau_i^{\tilde{c}_{2,d_{20}}} \cdot u^{*2} \quad (5)$$

$$d_{21} = c_{0,d_{21}} \cdot \tau_i^{\tilde{c}_{0,d_{21}}} + c_{1,d_{21}} \cdot \tau_i^{\tilde{c}_{1,d_{21}}} \cdot u^* \quad (6)$$

$$d_{22} = c_{0,d_{22}} \cdot \tau_i^{\tilde{c}_{0,d_{22}}} + c_{1,d_{22}} \cdot \tau_i^{\tilde{c}_{1,d_{22}}} \cdot u^* \quad (7)$$

140 with $c_{0,d_{20}} = 0.024$, $\tilde{c}_{0,d_{20}} = -0.0001$, $c_{1,d_{20}} = 0.0002$, $\tilde{c}_{1,d_{20}} = 1.076$, $c_{2,d_{20}} = 1.573$, $\tilde{c}_{2,d_{20}} = 1.622$, $c_{0,d_{21}} = 0.002$, $\tilde{c}_{0,d_{21}} = -0.001$, $c_{1,d_{21}} = 1.104$, $\tilde{c}_{1,d_{21}} = 1.395$, $c_{0,d_{22}} = 0.042$, $\tilde{c}_{0,d_{22}} = 0.002$, $c_{1,d_{22}} = 0.555$, $\tilde{c}_{1,d_{22}} = 0.364$.

Page 9, figure 3: On Page 7, line 156 the authors write that the drift and diffusion terms should be polynomials of order 2 and 3. Provide fits in figure 3 to illustrate this.

145

Added accordingly.

Page 9, equation 19: Do not put ‘exp’ in italics.

150

Changed accordingly.

Page 10, figure 4: The black-on-black isoline notations are virtually impossible to read.

Changed accordingly.

155

Page 10, figure 4: The math in the right panel does not look convincing. Can the authors comment on this?

As the estimation of the conditional pdfs is purely based on measurement data, sparse regions in the phase space will naturally result in poor estimations of pdfs. This is of course a major problem for our method, as it relies on those pdfs. With the plot in the right panel we wanted to show that we now can extrapolate conditional pdfs to sparse regions via numerical solutions of the Fokker-Planck equations. Still, even though the estimated conditional pdf suffers from a low availability of data, our numerical solution appears to be a reasonable representation of the true pdf. To make our approach clear, we added in the manuscript the comment: ‘Note that due the use of the FPE, the obtained pdfs are less noisy and extend to large values as seen in fig. 4’

165

Page 13, line 227: Typo: replace sigma with “sigma.”

Changed accordingly.

170

Page 13, line 227: Why can the coefficients D be considered slowly changing functions? Figure 7 seems to show the contrary.

In Figure 7 we show the timeseries of the wind speed fluctuations u^* , which are indeed fast-changing. Also the underlying conditional pdfs $p(u^*|u_1; \dots; u_N)$, shown to the right, are fast-changing, due to different values of u_1, \dots, u_N . It is a central point of our multipoint approach that the underlying Fokker-Planck equation, defined by its coefficients $D^{(i)}$, is not changing for this interval, or, respectively, is slowly changing due to the non-stationary nature of windspeeds. This slow change takes place on large time scales for which the mean values like \bar{U} are defined. In the same sense the joint pdfs $p(u^*; u_1, \dots; u_N)$ are changing only slowly, while the fast-fluctuating conditional pdfs $p(u^*|u_1; \dots; u_N)$ are generated by the fast-fluctuating arguments in the joint pdf. The basic difference is based on the aspect one is looking at. The signal is fast changing, but the underlying equation is fixed. Fast changes are generated by fast-fluctuating arguments of a slow-changing function.

Page 14, figure 8: Consider splitting the top panel into two. Through the overlapping curves, a lot of detailed information is getting lost.

Page 15, line 248: RANS should be spelled out.

Page 15, line 249: 'Great' is an odd choice of word.

Page 15, line 255: Consider rephrasing the sentence. Not all multipoint-based models automatically capture small-scale intermittency.

Page 15, line 265: Do not use capitals in the reference. Page 15, line 267: Capital 'A' in acknowledgments.

All changed accordingly.

Page 15, line 269: Is the first name of the person Andeé?

No, thank you for pointing this out.

Page 16 References: A lot of the references are inconsistent when it comes to providing doi, placement of first name letters and abbreviation dots.

Changed accordingly.

References

- Boettcher, F., Renner, C., Waldl, H.-P., and Peinke, J.: On the statistics of wind gusts, *Boundary-Layer Meteorology*, 108, 163–173, <https://doi.org/10.1023/A:1023009722736>, 2003.
- Morales, A., Waechter, M., and Peinke, J.: Characterization of wind turbulence by higher-order statistics, *Wind Energy*, 15, 391–406, <https://doi.org/10.1002/we.478>, 2012.
- Peinke, J., Tabar, M. R., and Wächter, M.: The Fokker–Planck Approach to Complex Spatiotemporal Disordered Systems, *Annual Review of Condensed Matter Physics*, 10, 107–132, <https://doi.org/10.1146/annurev-conmatphys-033117-054252>, 2019.

Reply to anonymous Referee No.2: Multipoint Reconstruction of Wind Speeds

Christian Behnken, Matthias Wächter, and Joachim Peinke

Institute of Physics/ForWind, University of Oldenburg.

Correspondence: Peinke (peinke@uni-oldenburg.de)

Copyright statement. TEXT

NOTE: All figure and equation numbers refer to the original submitted manuscript and may differ from the ones in the revised version.

- 5 **L13. I would argue that hydro is more represented in decarbonized energy sources than wind and solar; at least in some parts of the world. It should be included in this list.**

We added it to the list in the revised manuscript.

- 10 **L15. Why wind(solar) is capital in the manuscript?**

L25. The citation style is incorrect. Please revise accordingly.

L28. Should be “...known to be...”

L33. There should be a space between 10 and min. Please apply the same correction everywhere else (number and unit separation). Also, the citation style is incorrect. Please revise this issue everywhere in the manuscript.

15

All changed accordingly.

The exact definition of intermittency (for the context of this study) should be provided in the Introduction. The authors talk a lot about intermittency, but the exact definition is not provided.

20

We added following definition in the introduction:

“Within this context the term intermittency is used in the spirit of Kolmogorov 62 to describe the characteristic heavy-tailed shape of pdfs often found at small scales in time series of turbulent systems (Frisch, 2004).”

25 **L46. Remove one “and” at the end of this line.**

L60. It should be specified that t is the time.

L61–62. Please revise the sentence for proper English.

All changed accordingly.

30

L60 and L65. Please clarify the difference between $u(t)$ and $U(t)$.

We clarified it in the revised manuscript in the beginning of the method section:

35 “With $U(t)$ we refer to the resulting wind speed from the horizontal components. The quasi-stationary wind speed $u(t)$ is then obtained from $U(t)$ by respectively normalizing it with the mean \bar{U} and standard deviation σ_U within blocks of 1 min length.”

The abbreviation pdf is sometimes italicized and sometimes not. Please be consistent.

L110. There should be a comma after the Pawula theorem. Also, please provide a reference for this claim on L110 and L111.

40

All changed accordingly.

The reference for the Pawula theorem is Risken 1996. Regarding our claim in L110 und L111, we added following plot to the manuscript: “As one can see in fig. (1), the fourth Kramery-Moyal coefficient is slightly larger than zero, but negligible compared to the magnitude of the diffusion function $D^{(2)}$ ”

45

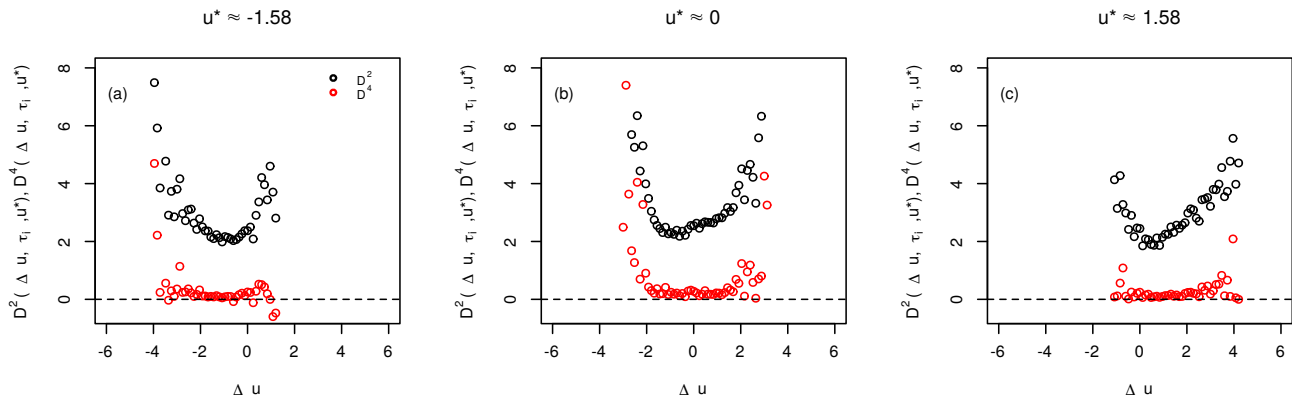


Figure 1. Exemplary estimations of the second and fourth Kramers-Moyal coefficient $D^{(2)}$ and $D^{(4)}$ for $\tau = 65$ s

L155–156. Why the order of the polynomial of 3 and 2. Is this the lowest polynomial order that properly fits the data?

Indeed third and second order polynomials for the drift $D^{(1)}$ and diffusion $D^{(2)}$ functions are the polynomials of lowest that are properly fitting the data. Empirical studies ((Renner et al., 2001), (Reinke et al., 2018)) suggests that these polynomials are well suited to problems in fluid mechanics. Choosing higher order polynomials is possible as well, but the parametrization might be suffering from overfitting then. Furthermore, up to now we did not see any fundamental changes in the results using higher order polynomials – see a rigorous approach to support these findings by the use of the integral fluctuation theorem for ideal turbulent data (Reinke et al., 2018).

Figure 2. The two labels in the legend are identical, but the different notation is used in the figure caption. Please correct this before this figure can be reviewed properly.

L167. Please correct the English.

All figures. Please add (a), (b), (c), etc. labels for subplots.

L179. I belie that “an” should be “a”.

Equation 19. The function \exp should not be italicized. The same holds for any other function in the manuscript.

L223. The word \min should not be italicized.

All changed accordingly.

MAJOR COMMENT: L226. In non-stationary wind speed records, the fluctuations are dependent on wind speed. Reading this section (and this particular line), this reviewer concludes that the presented methodology does not account for this relationship. For instance, in the case of non-stationary thunderstorm winds, Chen and Letchford (2004) (doi: 10.1016/j.engstruct.2003.12.009) modulated the fluctuations based on the moving-mean wind speed. A similar approach was used by Chay et al. (2004) (doi: 10.1016/j.engstruct.2005.07.007). This has been shown on the example of full-scale data of thunderstorm winds in Burlando et al. (2017) (doi:10.1175/MWR-D-17-0018.1) and Zhang et al. (2018) (doi: 10.1016/j.probengmech.2017.06.003). Notice that in these papers the moving-mean turbulence intensity in the transient (thunderstorm) wind record is not changing in time. This confirms that the fluctuations increase as the mean wind speed increases. Please clarify this issue because it is particularly important for transient wind speed records. This change (previous comment) would perhaps correct for the discrepancies between the measurements and the reconstruction in Figure 8 (pdfs).

This comment of the referee addresses several points to which we want to answer:

Comment on Chen and Letchford (2004) (doi: 10.1016/j.engstruct.2003.12.009): In this paper special wind situations of thunderstorm downbursts are grasped by a deterministic–stochastic hybrid model. The fluctuation is modeled as a uniformly

modulated evolutionary vector stochastic process. In our paper we focus on this stochastic part and not on the larger scale deterministic part as (Chen and Letchford, 2004). In contrast to (Chen and Letchford, 2004) we do not model the fluctuations by a stochastic process in time, but we show that a new class of a sstochastic process in scale can be used. Common stochastic processes are Markovian in time and thus are not able to grasp general aspects of multi-point statistics. Turbulent wind signals
85 are in general not Markovian in time, but it is the novelty that we show in our paper that these turbulent wind fluctuations are Markovian with respect to a special scale process (see fig. 2), which enables us to set up a stochastic process in scale. This scale process is more complicated, but statistically more complete.

Cases of rapidly changing wind conditions like thunderstorm events or other transient wind speed changes are not
90 **in the focus of our work.** We aim at modelling the quasi-stationary wind speed fluctuations $u^*(t)$, which are obtained by a blockwise normalization (of 1 min length) with respect to the mean and standard derivation of wind speeds $U(t)$. This way we decouple the fluctuations from the magnitude of the mean flow. As stated later on, a rescaling of the fluctuations is achieved when we transform the modelled fluctions $u^*(t)$ back to real wind speeds U^* , by multiplying it with the standard derivation:
$$U^* = (\sigma_U \cdot u^*) + U.$$

95 If and how our approach may be adapted to situations like thunderstorms is out of the scope of our paper, may be just a shortening of our decomposition in 1 min - blocks is already helpful. We would agree to add this point as a fotenote in our paper or add it to the discussion.

Concerning the discrepancy of Fig 8:

100 In our data there was no thunderstorm like behavior. The discrepancy is mainly statistical nature. We have two comments to the discrepancies in the plots of fig. 8:

- a) Discrepancy in the timeseries: The mean wind speeds $\bar{U}(t)$ were generated by simple stochastic model and thus there will be deviations from the corresponding mean wind speeds from the measurements to the very same timestamp. If we would have used the historic mean wind speeds, there would be only minor deviations.
- 105 b) Discrepancy in the increment pdfs: The main deviations in the incrementd pdfs are found at the tails of the pdf on larger scales τ_i (note also the logarithmic y-scale). As these are probabilities our model is virtually completely correct for all scales, especially for small scales τ_i .

MAJOR COMMENT: Related to my previous comment, non-stationary velocity records are often non-Gaussian too. Can you please clarify how is this accounted for in your methodology?

110

This is correct. The central point for our approach here is the validity of the Markov property. If this is fulfilled, the other parts, like the shape of the probability distributions, are mathematically rigorous consequences. As mentioned above, in a careful investigation one may find wind conidations for which our approach is not valid. The importance of such cases are out of

the scope of our work presented here.

115

MAJOR COMMENT: The purpose of this methodology is to generate fluctuating wind records. This topic addressed in the seminal paper by Shinozuka (1972) (doi: [https://doi.org/10.1016/0045-7949\(72\)90043-0](https://doi.org/10.1016/0045-7949(72)90043-0)). Without going into mathematical rigor in this review, the basis of his method is to generate random numbers (through Monte Carlo) that follow the prescribed power spectral density of wind fluctuation (e.g., Kamal spectra, Davenport spectra, von Karman spectra, Mann spectra, etc.). This method is later implemented in some of the studies provided in my comment 20 and references therein. So, my question is how the method proposed in your study extends beyond this well-established methodology of generating wind fluctuations? What are the benefits of using the presented method in your study?

Methods relying on a prescribed power spectral density (PSD) to generate time series of wind speed fluctuations do have the benefit of being computationally fast and applicable without posing much requirements on the data. Nevertheless such methods only provide time series of a predefined length as shown for the amplitude-modulation scheme in (Chen and Letchford, 2004). The benefit of our method is that a time series can be continued in-situ for an arbitrary amount of iterations. Due to the stochastic nature of our algorithm an ensemble of possible scenarios for the evolution of the wind speed fluctuations, starting from a specific situation, can be assembled.

Furthermore, the main point of our paper is that we are mathematically much more general as Kamal spectra, Davenport spectra, von Karman spectra and Mann spectra, which are all low order two point (two time quantities, (see (Peinke et al., 2019))). Thus intermittency (higher order two point quantity) like fig. 8 and more complex multipoint structures (like gusts, see fig. 7) are now grasped by our approach. Our paper will open a new way to investigate such data (see (Fuchs et al., 2020) and (Hadjihosseini et al., 2016)). Note that the knowledge of the Fokker-Planck equation describes in a very compact way all the changes in statistics of two point (time) quantities as shown in fig 8.

MAJOR COMMENT: Can the authors plot spectra of the two velocity time series in Figure 5? Please also include the reference $-5/3$ slope for benchmarking.

We see a good agreement between the spectra from the measurements and the reconstruction with the $-5/3$ spectra within the internal subrange between $f > 0.1 Hz$ and $f < 1 Hz$ (see fig. 2). The flattening of the spectra observed at low frequencies ($f < 0.1 Hz$), was also noted by (Morales et al., 2012) for wind speeds in a similar range. But as this observation is not of interest for our work, we do not discuss further details here.

Furthermore we would like to stress that the spectrum from the reconstructed time series matches the one from the measurement very well, disregarding the deviations at high frequencies, where we are in the range of measurement noise of the ultrasonic anemometer. This shows that our method is able to capture two-point statistics like the power spectral density, but we would like to note, that we are going beyond, as the generated wind speed fluctuations $p(u^*, t^* | u_1, t^* - \tau_1; \dots; u_N, t^* - \tau_N)$ are based

on N-point statistics.

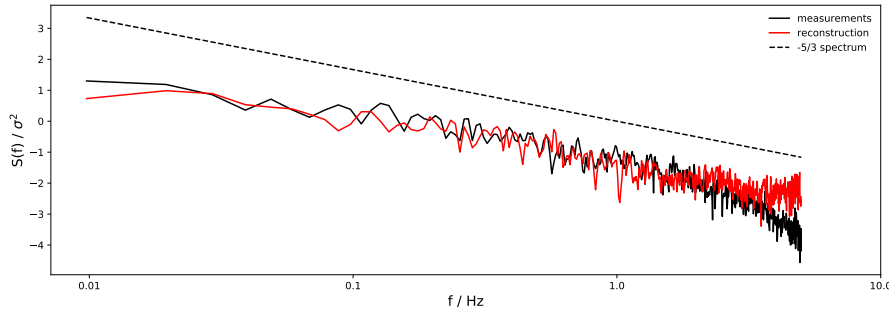


Figure 2. power spectral density of measured and reconstructed wind speed fluctuation

150 **MAJOR COMMENT: Going back to L36 in the Introduction. The authors correctly talk about the spatial dependency of fluctuations and coherence. How is the current model generating fluctuations in space? The presented results are for a point measurement, but the implementation for wind energy (i.e., wind turbine) analysis requires the spatially dependent profile. How a coherence function can be implemented in the method?**

155 The main scope of our paper is to present a new method to generate realistic time series of wind speed fluctuations. An extension to higher dimensions, enabling one to generate wind fields in time and space is of course desirable, but the authors would consider this to be the next step, as this will not be straightforward to do. We have three further remarks on our approach:

- a) The one-point time signal corresponds in the common approach of Taylor's frozen turbulence hypothesis to spatial structures in the flow direction, regardless some necessary correction to Taylor's hypothesis.
- 160 b) Our approach is statistically complete for one direction (in the sense of grasping any n-point statistics), thus the question to extend this to the full three-dimensional space would run into a statistical solution of the turbulence problem, which is still our dream to pave the way.
- c) The knowledge of a one point-time series already provides a better prediction of loads and power outputs as shown by (Wächter et al., 2010)

165

L238. The phrase "a fairly nice match" is not scientific. Please be specific.

We reformulated our comparison in the revised manuscript.

170 **How computationally efficient is your method? How much computational time is required to generate a fluctuation time series of different lengths? Can you please comment on this?**

One step in scripting languages like Python or R takes on average about 0.0005 s at generating a time series of 10^4 length on an ordinary PC. Utilizing languages like C/C++ or Fortran the computation should be boosted at least with a factor 10-100.
175 So the decline in processor power upon generating very large time series will not be of much impact for the practicability of our method. It is also not the computational efficiency which we emphasize here, but the new quality (multi-point statistics) we give access to by this approach.

L252–L253. Not necessarily until the method accounts for the spatially coherent fluctuations.

180 We agree that this is an important aspect. Thus we suggest to add a footnote in our article to clarify this point:
“Note, here we do not include the aspect of spatial coherence. To affect a big WEC such temporal fluctuations must have a sufficient large spatial structure.”

References. Some citations include article titles while the others do not. In addition, some journal names are abbreviated whereas the others are not. Please be consistent.
185

Changed accordingly.

Title: what exactly the authors mean by “multipoint?” This reviewer assumes this word signifies the time dependency of the methodology. If yes, isn’t this redundant because fluctuations have to be time dependent?
190

We agree that the term “multipoint” needs to be specified. We will add following explanation in the introduction:
“While commonly applied methods, like spectral analysis and two-point correlations, limit themselves to two-point statistics, here we extend the methodology to more than two points in time. We obtain generalized correlations between multiple points in time, in terms of probability density functions (pdfs) for the occurrence of a whole sequence of wind speeds. Those pdfs we denote multipoint pdfs, and they constitute the basic concept of our approach.”
195

References

- Chen, L. and Letchford, C. W.: A deterministic–stochastic hybrid model of downbursts and its impact on a cantilevered structure, *Engineering Structures*, 26, 619–629, <https://doi.org/10.1016/j.engstruct.2003.12.009>, 2004.
- 200 Frisch, U.: *Turbulence: The Legacy of A. N. Kolmogorov*, vol. 1, Cambridge Univ. Press, 2004.
- Fuchs, A., Queirós, S. M. D., Lind, P. G., Girard, A., Bouchet, F., Wächter, M., and Peinke, J.: Small scale structures of turbulence in terms of entropy and fluctuation theorems, *Phys. Rev. Fluids*, 5, 034 602, <https://doi.org/10.1103/PhysRevFluids.5.034602>, 2020.
- Hadjihosseini, A., Wächter, M., P.Hoffmann, N., and Peinke, J.: Capturing rogue waves by multi-point statistics, *New J. Phys*, 18, 013 017, 205 <https://doi.org/10.1088/1367-2630/18/1/013017>, 2016.
- Morales, A., Waechter, M., and Peinke, J.: Characterization of wind turbulence by higher-order statistics, *Wind Energy*, 15, 391–406, <https://doi.org/10.1002/we.478>, 2012.
- Peinke, J., Tabar, M. R., and Wächter, M.: The Fokker–Planck Approach to Complex Spatiotemporal Disordered Systems, *Annual Review of Condensed Matter Physics*, 10, 107–132, <https://doi.org/10.1146/annurev-conmatphys-033117-054252>, 2019.
- 210 Reinke, N., Fuchs, A., Nickelsen, D., and Peinke, J.: On universal features of the turbulent cascade in terms of non-equilibrium thermodynamics, *J. Fluid Mech*, 848, 117–153, <https://doi.org/10.1017/jfm.2018.360>, 2018.
- Renner, C., Friedrich, R., and Peinke, J.: Experimental indications for Markov properties of small-scale turbulence, *J. Fluid Mech*, 433, 383–409, <https://doi.org/10.1017/S0022112001003597>, 2001.
- Wächter, M., Mücke, T., and Peinke, J.: Influence of vertical shear and turbulence intensity on Langevin power curves, *DEWEK Bremen*, 215 2010.

Multipoint Reconstruction of Wind Speeds

Christian Behnken, Matthias Wächter, and Joachim Peinke

Institute of Physics/ForWind, University of Oldenburg.

Correspondence: Peinke (peinke@uni-oldenburg.de)

Abstract. The most intermittent behavior of atmospheric turbulence is found for very short time scales. Based on a concatenation of conditional probability density functions (cpdfs) of nested wind speeds increments, inspired by a Markov process in scale, we derive a short-time predictor for wind speed fluctuations around a non-stationary mean value and with a corresponding non-stationary variance. As a new quality this short time predictor enables a multipoint reconstruction of wind data. The used cpdfs are (1) directly estimated from historical data from the offshore research platform FINO1 and (2) obtained from numerical solutions of a family of Fokker-Planck equations in the scale domain. The explicit forms of the Fokker-Planck equations are estimated from the given wind data. A good agreement between the statistics of the generated synthetic wind speed fluctuations and the measured is found even on time scales below 1s. This shows that our approach captures the short-time dynamics of real wind speed fluctuations very well. Our method is extended by taking the non-stationarity of the mean wind speed and its non-stationary variance into account.

Copyright statement. TEXT

1 Introduction

The transition of our energy system, formerly strongly relying on gas and coal, to a decarbonized one, mainly based on wind and solar, solar and as well hydro power, is still ongoing work, but great progress has been made: From 2005 to 2017 the share in installed capacity of Wind (Solar wind (wolar)) has been increased from 6% (0.3%) to 18% (11.5%) in the European Union (WindEurope, 2018). The downside of this increasing share of those fluctuating renewable energy sources is their integration into the power grid. By analyzing measurements of fed-in wind and solar power it could be shown that their fluctuations strongly deviate from Gaussian behavior on time scales ranging from hours to seconds (Anvari et al., 2016) and for wind power even for scales below 1s (Haehne et al., 2018). This survival of the atmospheric intermittency in the power grid faces the grid operators with the great challenge to ensure stable power supply, even under highly volatile conditions. Within this context the term intermittency is used in the spirit of Kolmogorov 62 to describe the characteristic heavy-tailed shape of pdfs often found at small scales in time series of turbulent systems (Frisch, 2004).

To aid the design of our future energy systems, for example to size the needed energy storage or the power generation capacity of conventional power plants, much work has been done in the field of long term wind speed/power modeling, utilizing Markov

25 chain models. Whereas simple first-order Markov chain models cannot grasp the characteristics of long term correlations of wind speeds (K and L, 2009), higher-order Markov chain models perform better, but will require more input data for estimating the transitions matrices or some simplifications ((Pesch et al., 2015), (K and L, 2009), (Papaefthymiou and Klockl, 2008), (Weber et al., 2018)).

Despite their dramatic effect of long range correlation and fluctuations of wind speeds on the power generation (and thus the grid stability), wind speed fluctuations are known to be most intermittent on short time scales (Boettcher et al., 2003). With short time scales we refer to time scales in the range of seconds to minutes. As it can be seen in (Boettcher et al., 2003). The effect of intermittency is most prominent at time scales < 1 s, but as the time scales increase, the pdfs broaden. Models considering time steps ranging from minutes to seconds or even below are of course not suited for energy system analysis on national levels, but are useful tools for wind turbine operators. For a time step of ~~10min~~ 10 min (Carpinone et al., 2010) presented a higher-order Markov chain model for wind power and (Milan et al., 2013) showed a stochastic power model based on a conditional Langevin equation to work even in the range of seconds.

The knowledge of full three-dimensional wind fields for all three velocity components and the pressure in all details would be desirable. The missing of the basic understanding, the impracticability of handling such huge data sets as well as the complexity of the wind energy conversion process leads often to the demand of simplified models for wind speed. Common approaches for the design of wind turbines are the so-called Mann uniform shear and the Kaimal spectral and exponential coherence model (ie, 2005). Both models take spectral and coherence aspects of turbulent velocity fluctuations in account, thus handling the fluctuations as Gaussian distributed and stationary. Higher order statistical effects like the prominent intermittency effect of turbulence and non-stationarities are not taken into account, see for example (Mücke et al., 2011). Another approach is to use one-dimensional effective wind speed time series, representing for example the wind field together with the rotor aerodynamics as it impacts the drive train or can be used to model the above discussed energy conversion process (Wächter et al., 2011).

Within this work we propose a novel stochastic generator of one-dimensional wind speed fluctuations with a sampling interval of 0.1 s. One main novelty is that we show how to grasp by this model multipoint statistics of wind structures in time. While commonly applied methods, like spectral analysis and two-point correlations, limit themselves to two-point statistics, here we extend the methodology to more than two points in time. We obtain generalized correlations between multiple points in time, in terms of probability density functions (pdfs) for the occurrence of a whole sequence of wind speeds. Those pdfs we denote multipoint pdfs, and they constitute the basic concept of our approach. Such a stochastic multipoint approach should in principle be able to grasp wind structures like gust as well as clustering of wind fluctuations. The method was initially developed by (Nawroth and Peinke, 2006) in the context of homogeneous isotropic turbulence and later on applied to the modeling of log-return rates of current exchange rates (Nawroth et al., 2010) and ~~and~~ velocity increments of idealised homogeneous isotropic turbulence (Stresing and Peinke, 2010). The successful application to ocean gravity waves (Hadjihosseini et al., 2016) showed that structures of monster waves can be grasped by this approach correctly (Hadjihoseini et al., 2018). For a recent review see (Peinke et al., 2019). Finally we want to point out that we show also how to handle the aspect non-stationary wind conditions. We will continue as follows: In a first part we discuss the method for a subset of wind data characterised by its mean wind speed and its standard deviation. For such data it is shown how, arising from a Langevin process in a scale, a predictor for the

60 upcoming wind speed fluctuation around a mean value can be derived by a nesting of conditional probability density functions. Afterwards we check for Markovian properties of the wind speed fluctuations in scale and set up a Fokker-Planck equation, corresponding to the Langevin process in scale, and show how it contributes to the improvement of our stochastic prediction method. Finally in the second part the non-stationary mean wind speed and its non-stationary variance is incorporated into our approach to achieve more realistic wind speed time series.

65 2 Method

In this section we present the stochastic framework used for our multipoint reconstruction scheme. As a simplification we start this discussion for ~~1 min~~-blocks of wind data $U(t)$ - $U(t)$, with the time t , which share the same mean wind speed \bar{U} and the same standard deviation σ_U , as suggested in (Morales et al., 2012)(Morales et al., 2012). Fixing \bar{U} and σ_U -we generate quasi-stationary- σ_U one would generate quasi-stationary subsets of data. ~~As data we~~ We follow this idea, but instead of creating quasi-stationary subsets, we aim at creating quasi-stationary time series. With $U(t)$ we refer to the resulting wind speed from the horizontal components. The quasi-stationary wind speed $u(t)$ is then obtained from $U(t)$ by respectively normalizing it with the mean \bar{U} and standard deviation σ_U within blocks of 1 min length. We use measured data from the offshore research platform FINO 1: The data were recorded at a sampling frequency of 1 Hz between calendar week 1 to 10 in 2007 by-with an ultrasonic anemometer, mounted at ~~80m height~~80 m height, resulting in approximately $6 \cdot 10^6$ samples. The use of ~~the methods~~ our method for non-stationary time series is outlined in Section 3. ~~Concerning the notations, we abbreviate in this Section stochastic notations like $p_{\bar{U}, \sigma_U}(\dots)$ by $p(\dots)$, i.e. the discussion is implicitly restricted to these block condition. The wind speed of such a block sequence is labeled by $u(t)$, here u is normalised to zero mean and standard deviation of 1.~~

2.1 Multipoint Statistics

Since we assume wind speeds to emerge from a turbulent cascade, increments will take a key role for our method. Having a time series of wind speeds $u(t)$, the corresponding increment time series $\Delta u(\tau)$, depending on a certain scale τ , is given by

$$\Delta u(\tau) = u(t) - u(t - \tau). \quad (1)$$

This is the definition of so called right-sided increments. Note that the calculation of $\Delta u(\tau)$ after this definition depends on the current wind speed $u(t)$ and a past value $u(t - \tau)$, whereas the use of left-sided increments $\Delta u(\tau) = u(t + \tau) - u(t)$ would premise the knowledge of future values $u(t + \tau)$, creating a contradiction as we aim at producing synthetic wind speed time series. To ease readability we use the shorthand notations $u_i := u(t - \tau_i)$ and $\Delta u_i := u(t) - u(t - \tau_i)$ with $\tau_i = i \cdot \tau$ ($i = 1, 2, 3, \dots$) in the following.

As a further remark we note that although we consider in this work time series of wind speed, we often talk of multipoint statistics. $\Delta u(\tau)$ is considered as a statistical two-point quantity, which more correctly could be denoted as two-time quantity. Based on the commonly used hypotheses on frozen turbulence by Taylor, for short time fluctuations time and space statistics are related linearly by the mean wind speed (see also (Peinke et al., 2019)).

Our idea is to predict a wind speed $u^*(t^*)$ only by knowledge of its N past values $\{u_1(t^* - \tau_1), \dots, u_N(t^* - \tau_N)\}$. The probability of an event u^* to happen at time t^* can then be expressed by the conditional probability density function (**conditional pdf/cpdf**)

$$p(u^*, t^* | u_1, t^* - \tau_1; \dots; u_N, t^* - \tau_N) = \frac{p(u^*, t^*; u_1, t^* - \tau_1; \dots; u_N, t^* - \tau_N)}{p(u_1, t^* - \tau_1; \dots; u_N, t^* - \tau_N)}, \quad (2)$$

95 using the definition of conditional probabilities. Note this **conditional pdf/cpdf** is the key quantity to estimate a new wind speed value u^* and it can be used iteratively to generate new time series, as we show below.

~~To link equation (2) to the idea of an underlying turbulent cascade we identify the conditional pdf on the lhs with the conditional pdf $p(u^*, t^* | \Delta u_1, t^* - \tau_1; \dots; \Delta u_N, t^* - \tau_N)$. Thus the numerator of the rhs of (2) can be rewritten as~~

$$\frac{p(u^*, t^*; u_1, t^* - \tau_1; \dots; u_N, t^* - \tau_N)}{p(u^*, u^* - u_1, \tau_1; \dots; u^* - u_N, \tau_N)}$$

100 ~~and the nominator as~~

$$\frac{p(u_1, t^* - \tau_1; \dots; u_N, t^* - \tau_N)}{p(u_1; u_1 - u_2, \tau_2 - \tau_1; \dots; u_1 - u_N, \tau_N - \tau_1)}$$

~~The identity of the expressions in (A1) and (A2) can mathematically rigorously be shown, as done in (Nawroth et al., 2010), but intuitively speaking the sequences on the lhs and rhs must yield the same joint pdf, since the increments on the rhs respectively have a common reference point u^* or u_1 . Next we factorize the joint pdfs from equations (A1) and (A2) by iteratively using~~

105 ~~conditional pdfs~~

$$\frac{p(u^*; \Delta u_1, \tau_1; \dots; \Delta u_N, \tau_N)}{p(\Delta u_1, \tau_1 | \Delta u_2, \tau_2; \dots; \Delta u_N, \tau_N; u^*) \cdot p(\Delta u_2, \tau_2 | \Delta u_3, \tau_3; \dots; \Delta u_N, \tau_N; u^*) \cdots p(\Delta u_{N-1}, \tau_{N-1} | \Delta u_N, \tau_N; u^*) \cdot p(\Delta u_N, \tau_N | u^*) \cdot p(u^*)}$$

~~and with $\tilde{\Delta} u_i := u(t^* - \tau_1) - u(t^* - \tau_i)$ with the time scale $\tilde{\tau}_i :=$~~

$$\frac{p(u_1; \tilde{\Delta} u_2, \tau_2 - \tau_1; \dots; \tilde{\Delta} u_N, \tau_N - \tau_1)}{p(\tilde{\Delta} u_2, \tau_2 - \tau_1 | \tilde{\Delta} u_3, \tau_3 - \tau_1; \dots; \tilde{\Delta} u_N, \tau_N - \tau_1; u_1) \cdot p(\tilde{\Delta} u_3, \tau_3 - \tau_1 | \tilde{\Delta} u_4, \tau_4 - \tau_1; \dots; \tilde{\Delta} u_N, \tau_N - \tau_1; u_1) \cdots p(\tilde{\Delta} u_{N-1}, \tau_{N-1} - \tau_1 | \tilde{\Delta} u_N, \tau_N - \tau_1; u_1) \cdot p(\tilde{\Delta} u_N, \tau_N - \tau_1 | u_1) \cdot p(u_1)}$$

110 A further step in reducing the dimensionality of the involved pdfs can be performed upon assuming the scale process to be Markovian, i.e., which can be described by means of a Markov process. Thus we assume that there exists a time-scale separation $\Delta\tau_{ME} = \tau_j - \tau_i$ ($j > i$), where

$$p(\Delta u_i, \tau_i | \Delta u_j, \tau_j + \Delta\tau_{ME}; \dots; \Delta u_n, \tau_n + n \cdot \Delta\tau_{ME}; u^*) =$$

$$p(\Delta u_i, \tau_i | \Delta u_j, \tau_i + \Delta\tau_{ME}; u^*)$$

115 holds. The time after which the Markov condition is fulfilled for all greater scales. This scale separation $\Delta\tau_{ME}$ is often called the Markov-Einstein length (Einstein, 1905) and for various systems its existence could be shown empirically, ranging from jet streams in laboratory experiments (Renner et al., 2001), (?) to large geophysical systems such as ocean gravity waves (Hadjihosseini et al., 2016). It enables us to express the multiple cpdf $p(u^*, t^* | u_1, t^* - \tau_1; \dots; u_N, t^* - \tau_N)$ by a multiplication of simpler double cpdf and marginal pdfs:

$$p(u^*, t^* | u_1, t^* - \tau_1; \dots; u_N, t^* - \tau_N) =$$

$$\frac{p(u^*) \cdot \prod_{i=1}^{N-1} p(\Delta u_i | \Delta u_{i+1}; u^*) \cdot p(\Delta u_N | u^*)}{p(u_1) \cdot \prod_{i=2}^{N-1} p(\Delta u_i | \Delta u_{i+1}; u_1) \cdot p(\Delta u_N | u_1)}, \quad (3)$$

with $\tilde{\Delta}u_i := u(t^* - \tau_1) - u(t^* - \tau_i)$ with the time scale $\tau_i - \tau_1$. For details we refer the reader to the appendix A.

120

It is known that the evolution of conditional pdfs cpdfs of a Markov process can be described by the famous Kramers-Moyal expansion Risken (1996), which notes for our stochastic process in scale Δu_i

$$-\tau_i \frac{\partial}{\partial \tau_i} p(\Delta u_i | \Delta u_j; u^*) =$$

$$\sum_{n=1}^{\infty} \left(-\frac{\partial}{\partial \Delta u_i} \right)^n \left[D^{(n)}(\Delta u_i, \tau_i, u^*) p(\Delta u_i | \Delta u_j; u^*) \right], \quad (4)$$

requiring $\tau_j - \tau_i \geq \Delta\tau_{ME}$ and with the Kramers-Moyal coefficients $D^{(n)}$ being defined as

$$125 \quad D^{(n)}(\Delta u_i, \tau_i, u^*) =$$

$$\lim_{\Delta\tau \rightarrow 0} \frac{\tau_i}{n! \Delta\tau} \langle [\Delta u_i'(\tau_i - \Delta\tau, u^*) - \Delta u_i(\tau_i, u^*)]^n \rangle. \quad (5)$$

In contrast to the Kramers-Moyal expansion in time domain, a minus sign on the lhs of equation (4) has to be added for scale processes, since during evolution of the process the scale τ is decreasing. According to the Pawula theorem, the Kramers-Moyal coefficients vanish for $n \geq 3$, if $D^{(4)} = 0$ (Risken, 1996), thus the Kramers-Moyal expansion reduces to the Fokker-Planck equation (FPE)

$$130 \quad -\tau_i \frac{\partial}{\partial \tau_i} p(\Delta u_i | \Delta u_j; u^*) =$$

$$-\frac{\partial}{\partial \Delta u_i} \left[D^{(1)}(\Delta u_i, \tau_i, u^*) p(\Delta u_i | \Delta u_j; u^*) \right] +$$

$$-\frac{\partial^2}{\partial \Delta u_i^2} \left[D^{(2)}(\Delta u_i, \tau_i, u^*) p(\Delta u_i | \Delta u_j; u^*) \right], \quad (6)$$

with the drift function $D^{(1)}$, accounting for the deterministic evolution of the stochastic process, whereas the so called diffusion function $D^{(2)}$ scales the amplitude of the noise term of the corresponding Langevin equation

$$-\frac{\partial}{\partial \tau} \Delta u(\tau, u^*) = \frac{1}{\tau} D^{(1)}(\Delta u, \tau, u^*) + \sqrt{\frac{1}{\tau} D^{(2)}(\Delta u, \tau, u^*)} \cdot \Gamma(\tau) \quad (7)$$

with the Gaussian noise $\Gamma(\tau)$, fulfilling $\langle \Gamma(\tau) \rangle = 0$ and as well $\langle \Gamma(\tau) \Gamma(\tau') \rangle = 2\delta_{\tau\tau'}$. This equation directly describes the evolution of a single trajectory along the scale τ .

As it can be easily seen, the FPE can be used to determine the factorized pdfs from eq. (A3) and eq. (A4) if the process is Markovian and higher order Kramers-Moyal coefficients are zero. By inserting those expressions into eq. (2), we finally get

$$p(u^*, t^* | u_1, t^* - \tau_1; \dots; u_N, t^* - \tau_N) = \frac{p(u^*)}{p(u_1)} \cdot \frac{\prod_{i=1}^{N-1} p(\Delta u_i | \Delta u_{i+1}; u^*)}{\prod_{i=2}^{N-1} p(\Delta u_i | \Delta u_{i+1}; u_1)} \cdot \frac{p(\Delta u_N | u^*)}{p(\Delta u_N | u_1)}$$

This equivalence between a conditional pdf cpdf with N conditions and a nested chain of several conditional pdfs cpdfs with only two conditions, stemming from the three-point closure of a cascade process, is extremely helpful if one aims at estimating the pdfs from measurements, since the high dimensional pdfs in eq. (2) would require a tremendous amount of realizations in order to be estimated well. For a more detailed discussion of this multipoint approach we refer to (Peinke et al., 2019).

2.2 Preliminary Analysis of Wind Speed Data

Next we check if wind speed data are suitable for the reconstruction method just described. According to the rhs of equation (3) the estimation of the double conditioned pdfs cpdfs $p(\Delta u_i | \Delta u_{i+1}, u^*)$ is necessary. However, to reduce computational costs or, respectively, the number of data points, it would be much more convenient to use the single conditioned pdfs cpdfs $p(\Delta u_i | \Delta u_{i+1})$ by excluding the condition on the wind speed u^* to be predicted (Nawroth et al., 2010; Peinke et al., 2019) (Nawroth et al., 2010), (Peinke et al., 2019). Thus the equality

$$p(\Delta u_i | \Delta u_{i+1}; u^*) = p(\Delta u_i | \Delta u_{i+1}) \quad (8)$$

must hold. As it can be seen from fig. (1), eq. (8) holds for $u^* \approx 0$, but shows a significant shift for $u^* \approx 2.5$, therefrom we reason that the equality in equation (8) cannot generally be assumed, so we have to stick to the double conditioned pdfs cpdfs $p(\Delta u_i | \Delta u_{i+1}, u^*)$. Similar results have been reported for idealised turbulence (Stresing and Peinke, 2010) and sea waves (Hadjihosseini et al., 2016). On derivation of our final formula for reconstruction of time series (cf. eq (3) an essential step was to premise the underlying scale process to be Markovian. Thus it has to been shown that for $\Delta \tau = \tau_{i+1} - \tau_i \geq \Delta \tau_{ME}$

$$p(\Delta u_i | \Delta u_{i+1}; \dots; \Delta u_N; u^*) = p(\Delta u_i | \Delta u_{i+1}; u^*) \quad (9)$$

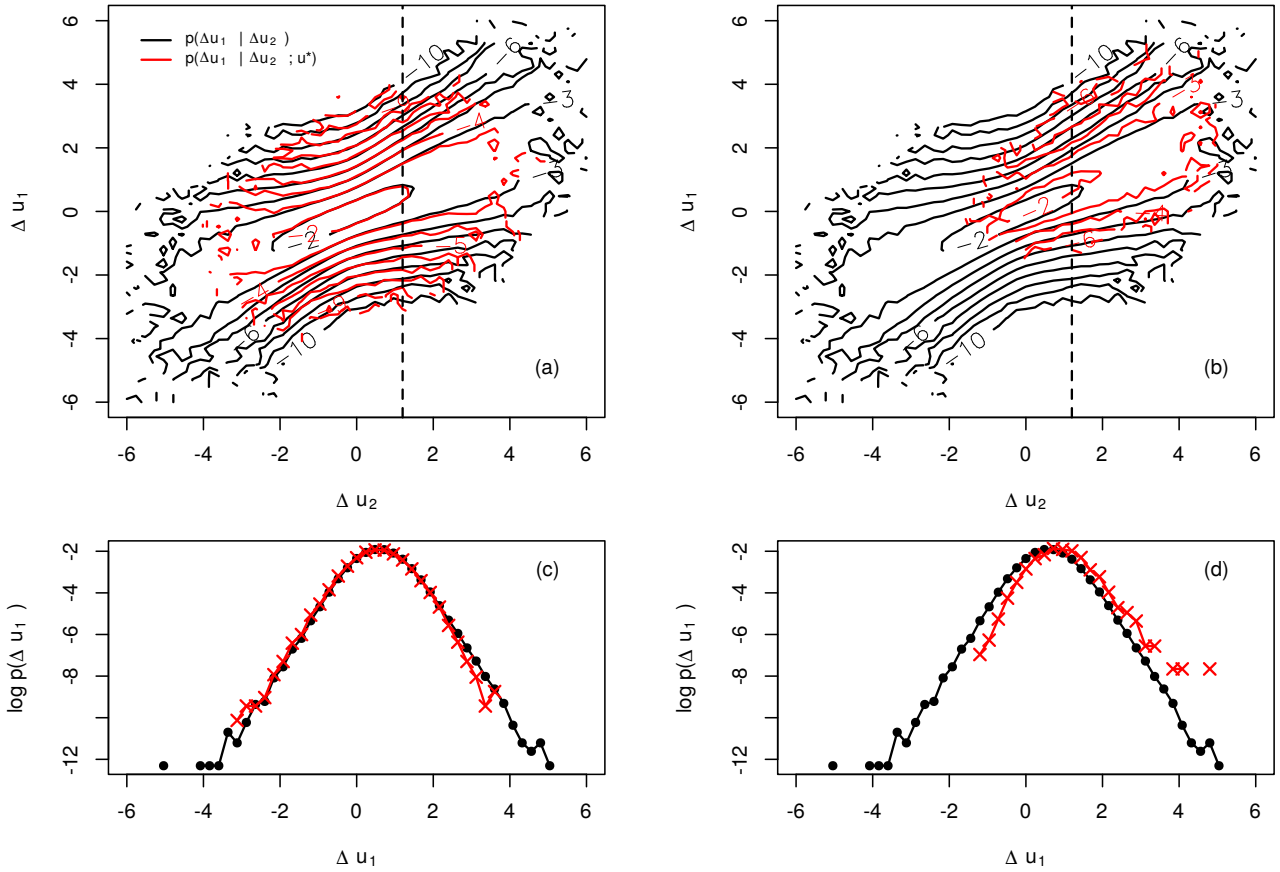


Figure 1. Comparison of single conditional pdfs $p(\Delta u_1 | \Delta u_2)$ (black) and double conditional pdfs $p(\Delta u_1 | \Delta u_2; u^*)$ (red) for $u^* \approx 0$ (left (a), (c)), $u^* \approx 2.5$ (right (b), (d)), $\tau_1 = 1s$ and $\tau_2 = 2\tau_1$. Dashed lines indicate cuts through the conditional pdfs at $\Delta u_2 \approx 1.2$. The levels of the contour plots are given in natural logarithmic scale.

is a valid assumption. As the verification of this expression is not feasible in its generality, we limit ourself by reducing the number of dimension involved and just check the equality of

$$p(\Delta u_i | \Delta u_{i+1}; \Delta u_{i+2}; u^*) = p(\Delta u_i | \Delta u_{i+1}; u^*). \quad (10)$$

To check this we utilize Chapman-Kolmogorov equation (CKE) (Friedrich et al., 2011): The conditional pdf $p(\Delta u_i | \Delta u_{i+2}; u^*)$ is estimated directly from observational data and afterwards compared with the conditional pdf $\tilde{p}(\Delta u_i | \Delta u_{i+2}; u^*)$ obtained numerically by use of the CKE

$$\tilde{p}(\Delta u_i | \Delta u_{i+2}; u^*) = \int p(\Delta u_i | \Delta u_{i+1}; u^*) p(\Delta u_{i+1} | \Delta u_{i+2}; u^*), \quad (11)$$

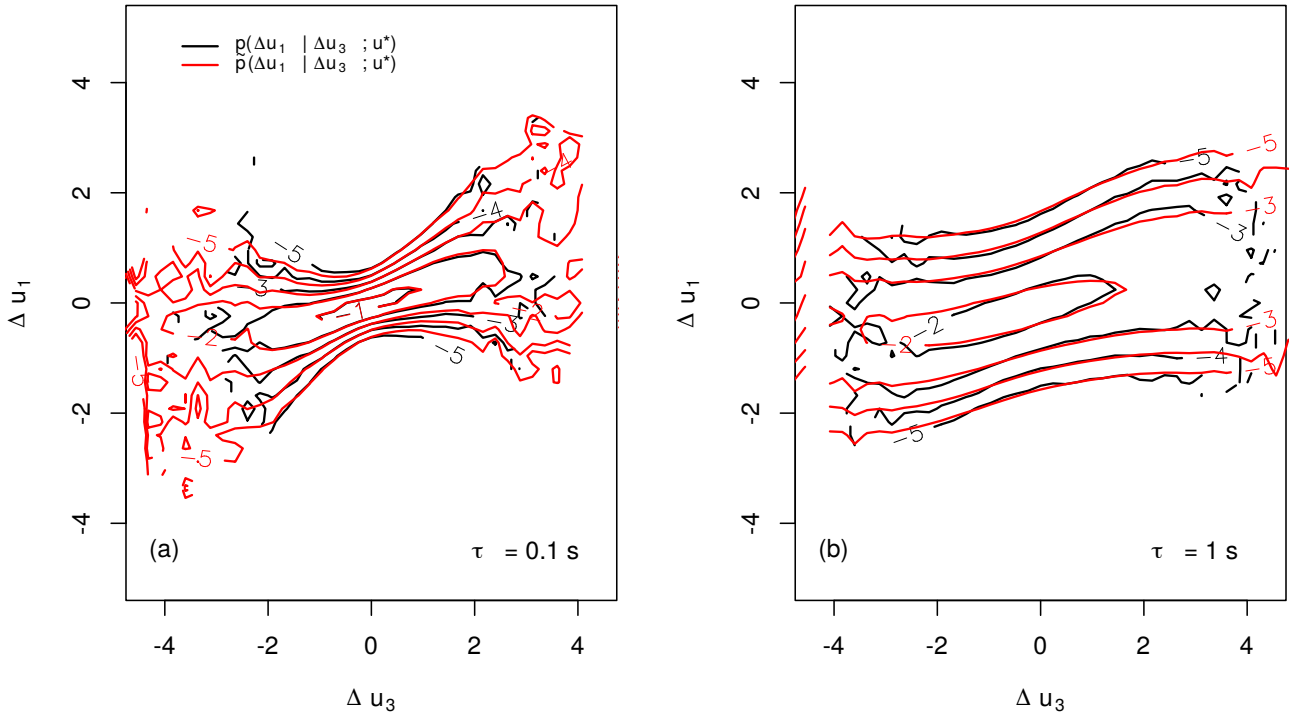


Figure 2. Comparison of the double [conditioned pdfs](#) $p(\Delta u_1 | \Delta u_3; u^*)$ (estimated from data) and $\tilde{p}(\Delta u_1 | \Delta u_3; u^*)$ (obtained from CKE) for $\tau_1 = 0.1$ s ([left](#)) or 1 s ([right](#)) and respectively $\tau_2 = 2\tau_1$, $\tau_3 = 3\tau_1$, $\Delta\tau = \tau_2 - \tau_1 = \tau_3 - \tau_2$ and $u^* = 0$.

whereas the two [conditional pdfs](#) within the integral on the rhs are as well directly estimated from data. Figure 2 shows that equation (11) only holds for $\Delta\tau \geq \Delta\tau_{ME}$. We find Markov-Einstein length $\Delta\tau_{ME} \leq 0.1$ s, which we are going to use henceforth.

2.3 Parametrization of the Fokker-Planck-Equation

As it was mentioned in sec. (2.1) the FPE may be used to generate solutions for the needed [conditional pdfs](#) in eq. (1). Aiming for this, one needs a parametrization of the FPE reflecting the scale process of the real world wind speed data. No general, physical formulation for a FPE, describing the scale process of wind speeds is known, thus we use the possibility to estimate a parametrization directly from the given data (cf. eq. (5) and ([Peinke et al., 2019](#))([Reinke et al., 2018](#); [Peinke et al., 2019](#))).

This way we get estimations of the drift and diffusion functions $D^{(1)}(\Delta u, \tau_i, u^*)$, $D^{(2)}(\Delta u, \tau_i, u^*)$ along the scale τ_i and for every wind speed value u^* . From these estimations one then usually finds parametrization of the FPE by fitting appropriate polynomial surfaces to the estimated functions, which then may be used to obtain numerical solutions of the FPE.

To match the functional shape of the estimated $D^{(1)}(\Delta u, \tau_i, u^*)$ and $D^{(2)}(\Delta u, \tau_i, u^*)$ (see fig. (3)) we require the polynomials

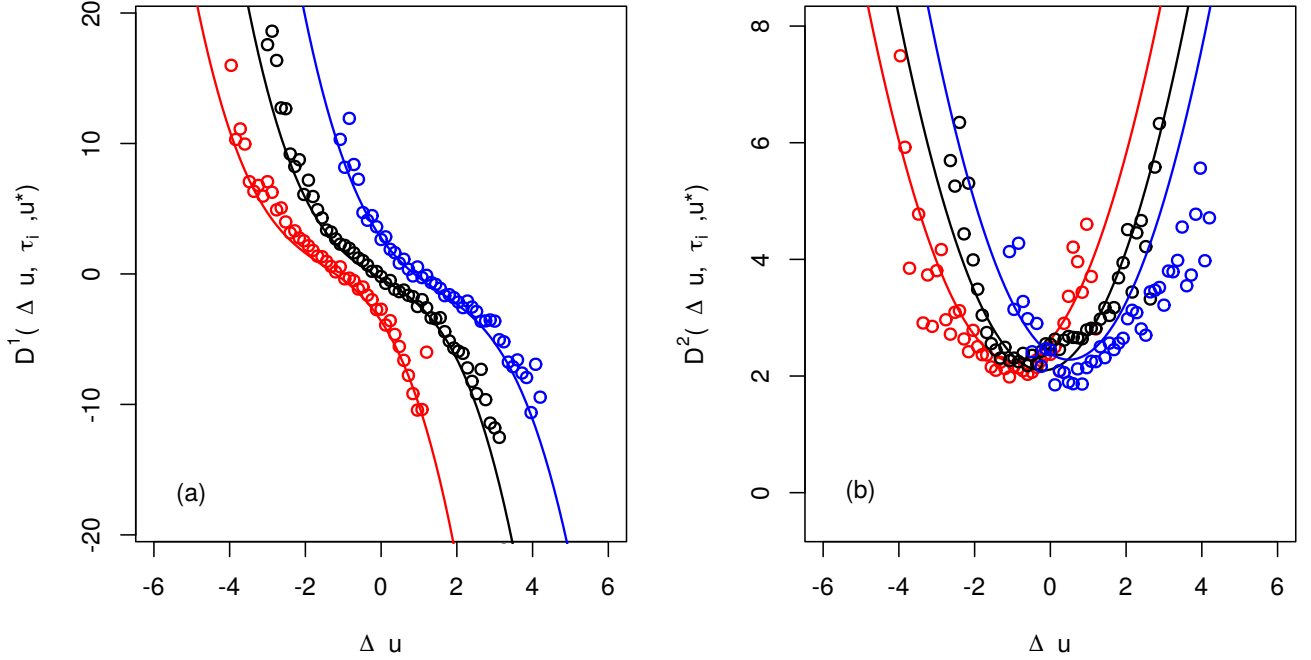


Figure 3. Exemplary estimations of the drift and diffusion functions $D^{(1)}(\Delta u, \tau_i, u^*)$, $D^{(2)}(\Delta u, \tau_i, u^*)$ for $\tau = 65$ s and $u^* \approx -1.58$ (red), ≈ 0 (black) and ≈ 1.58 (blue). [Fits for \$D^{\(1\)}\$ and \$D^{\(2\)}\$ were achieved by applying eq. \(12, 13\).](#)

to be of order 3 and 2 respectively. We find a significant shift $\gamma_{D^{(1)}, D^{(2)}}(\tau_i, u^*)$, denoted with $\gamma_{D^{(i)}}(\tau_i, u^*)$, depending on u^* and τ_i for ~~both drift and diffusion~~ the drift along all scales τ_i which has to be taken into account for a parametrization suitable to the given data.

180 We set for $D^{(1)}(\Delta u, \tau_i, u^*)$:

$$D^{(1)}(\Delta u, \tau_i, u^*) = d_{10}(\tau_i, u^*) + d_{11}(\tau_i, u^*) [u - \gamma_{D^{(1)}}(\tau_i, u^*)] + d_{13}(\tau_i, u^*) [u - \gamma_{D^{(1)}}(\tau_i, u^*)]^3 \quad (12)$$

and for $D^{(2)}(\Delta u, \tau_i, u^*)$:

$$D^{(2)}(\Delta u, \tau_i, u^*) = d_{20}(\tau_i, u^*) + d_{21}(\tau_i, u^*)u + d_{22}(\tau_i, u^*)u^2. \quad (13)$$

Similar findings were made for other system (Hadjhosseini et al., 2016) and (Stresing and Peinke, 2010), where the dependence on u^* was limited only to the drift function $D^{(1)}(\Delta u, \tau_i, u^*)$. For wind speed data the contribution of u^* is clearly more

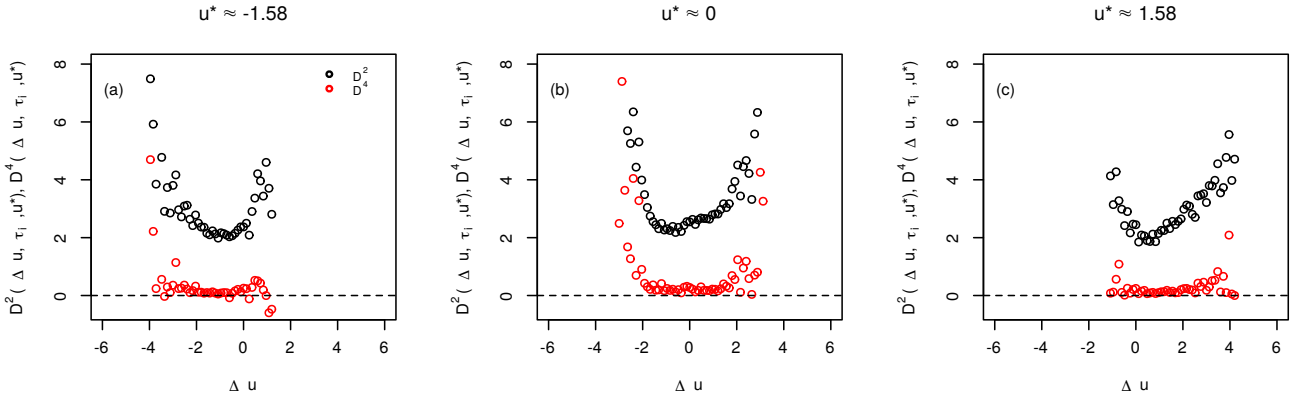


Figure 4. Exemplary estimations of the second and fourth Kramers-Moyal coefficient $D^{(2)}(\Delta u, \tau_i, u^*)$, $D^{(4)}(\Delta u, \tau_i, u^*)$ for $\tau = 65$ s

complex.

Furthermore we check the validity of the Pawula theorem, requiring $D^{(4)} = 0$. As one can see in fig. (4), the fourth Kramery-Moyal coefficient is slightly larger than zero, but negligible compared to the magnitude of the diffusion function $D^{(2)}$.

190 Next, we check if the parametrization of the FPE, given by the eq. (12) and (13) performs well in describing the underlying scale process, before one uses it for the reconstruction scheme presented in sec. 2.1. This can be easily be done by comparing conditional pdfs cpdfs estimated directly from the data and the ones obtained from numerical solutions of the FPE. The latter one is not carried out by common finite-difference schemes, but by an iterative approach (for first works see (Renner et al., 2001),(Wächter et al., 2003)). For an (very) small step size in scale $\Delta\tau$ the functions $D^{(1)}(\Delta u, \tau_i, u^*)$, $D^{(2)}(\Delta u, \tau_i, u^*)$ can
 195 assumed to be constant in τ , leading to an exact solution (cf. (Risken, 1996)) for the conditional pdf cpdf

$$p(\Delta u_j, \tau_j - \Delta\tau | \Delta u_i, \tau_i, u^*) = \frac{1}{2\sqrt{\pi D^{(2)}(\tau_i, u^*) \Delta\tau}} \exp \left[-\frac{(\Delta u_j - \Delta u_i - D^{(1)}(\tau_i, u^*) \Delta\tau)^2}{4D^{(2)}(\tau_i, u^*) \Delta\tau} \right], \quad (14)$$

describing the transition between wind speed increments of a larger scale τ_i to a smaller scale $\tau_i - \Delta\tau$. By iteratively combining this so called *short time propagator* (STP) with the CKE (see eq. 11) one is able to obtain conditional pdfs cpdfs $p(\Delta u_j, \tau_j | \Delta u_i, \tau_i, u^*)$ for arbitrary large scale differences $\tau_i - \tau_j \gg \Delta\tau$. In theory this procedure would lead to exact solutions of the FPE, but since one is limited to finite step sizes $\Delta\tau$, this methods of course only provides numerical approximations of the true conditional pdfs cpdfs.
 200

Comparing conditional pdfs cpdfs estimated directly from the data and from the numerical solution we see (fig. 5) that our proposed estimation in terms of $D^{(1)}(\Delta u, \tau_i, u^*)$ and $D^{(2)}(\Delta u, \tau_i, u^*)$ is well suited to describe the underlying scale process. Thus we use this parametrization for the reconstruction scheme.

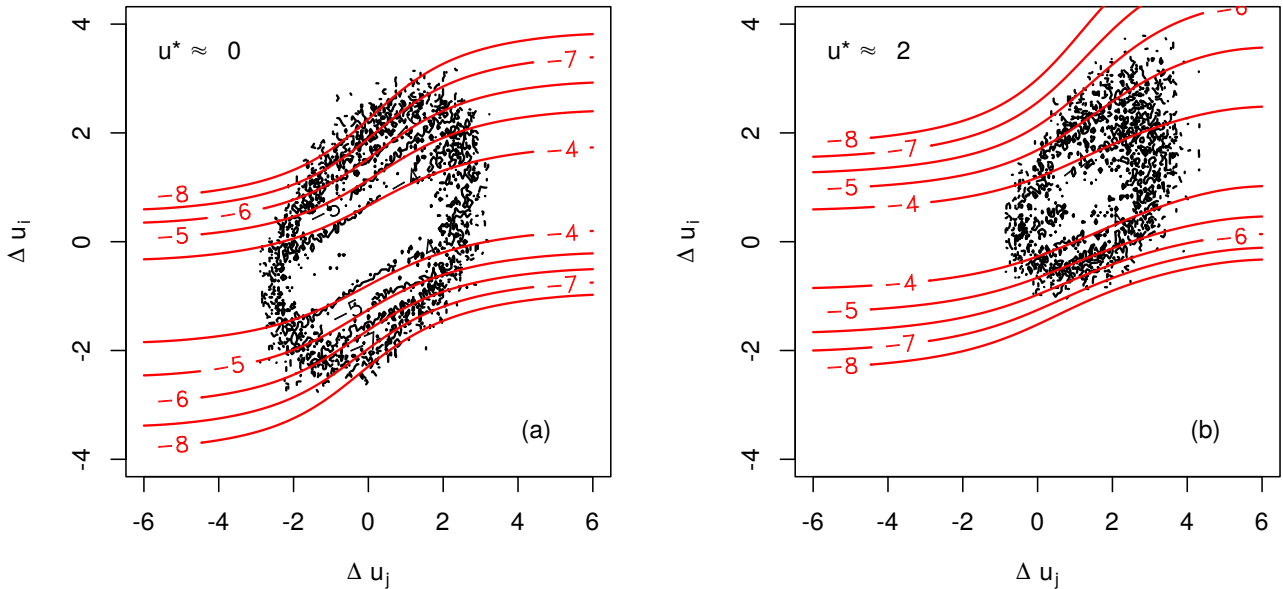


Figure 5. Isoline plots of a [conditional pdf](#) $p(\Delta u_i, \tau_i | \Delta u_j, \tau_j; u^*)$ estimated from the data (black) and from numerical solution of the FPE (red) for $\tau_i = 1.6$ s, $\tau_j = 3.2$ s and for $u^* \approx 0$ and $u^* \approx 2$

205 2.4 Results of the Multiscale Reconstruction

Alternatively to the presented approach to obtain the [conditional pdfs](#) from numerical solutions of the FPE, it is of course possible and much less cumbersome to estimate them directly from observational data. (Note [that due](#) the use of the FPEs, [the obtained pdfs are](#) less noisy and [extends](#) to large values as seen in fig. 5.) In this section we will present the results for the multipoint reconstruction achieved for u^* , yielding from both approaches.

210 To start the reconstruction scheme, we provided a short piece of the original time series of N wind speeds to the algorithm to compute the pdf $p(u^* | u_1, \dots, u_N)$, from which the first point of our simulation can be drawn. The reconstruction scheme is then shifted by one time step τ and applied again. By iteratively applying our method a new artificial time series of arbitrary length can be generated. After N iterations of the reconstruction scheme no data from measurements are required anymore to generate new values of u^* . From visual comparison in fig. 6 one finds a realistic looking simulated time series of u^* ,
 215 retaining the characteristics of dynamics on the smaller scales as well as the ones of the larger scales. To confirm this visual impression in a quantitative way, we compare the increment pdfs $p(\Delta u_i, \tau_i)$ obtained from the reconstructed and the measured time series. The synthetic time series were generated by using both, the [conditional pdfs](#) directly estimated from data and from numerical solutions of the PFE. As shown in fig. 7 the increment pdfs yielding from both stochastic simulations

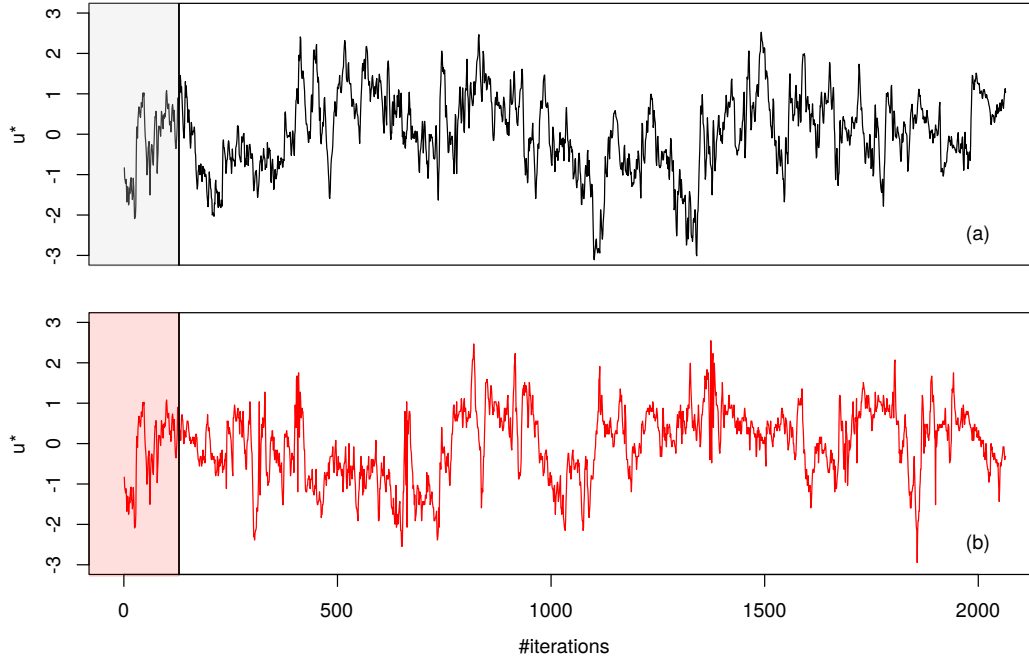


Figure 6. Comparison of original wind speed time series u^* (black, [upper picture \(a\)](#)) with the reconstructed one using eq. 8 (red, [lower picture \(b\)](#)). The vertical line marks the transition from the $N = 128$ on a logarithmic scale points provided as starting value for the reconstruction scheme to the simulated wind speeds.

nicely coincide with the pdfs from observations. This attests that the presented reconstruction scheme is able to capture the
 220 complex dynamics of wind speeds, characterized by a gradual shift of increment pdfs of a Gaussian-like shape (larger scales)
 to increment pdfs of heavy-tailed shape (smaller scales).

A striking difference between the increment pdfs from the stochastic simulation can be noted: Whereas the tails of the original
 pdfs are systematically underestimated by the reconstruction using the directly estimated pdfs, the reconstruction from the
 numerically obtained [conditional pdfs-cpdfs](#) is able to keep track of the tails of the original pdf. This stems from the fact,
 225 mentioned above, that by estimating a pdf from observational data one in general underestimates the outer tails, since there
 are only few measured points available. Considering the estimation of [conditional pdfs-cpdfs](#) the estimation error of course
 worsens, which is even more severe when additional conditioning is applied, like in our case in terms of the additional condition
 on u^* .

The tails of [conditional pdfs-cpdfs](#) $p(\Delta u_i, \tau_i | \Delta u_j, \tau_j; u^*)$ computed from the family of FPEs can be extrapolated to areas where
 230 no measurement points are available. This effect is a direct consequence of the CKE (11), as the tails are the product of quite
 well estimated less probable but not rare events.

Certainly this approach indirectly suffers from the limited number of observations as well, as the estimation of the function

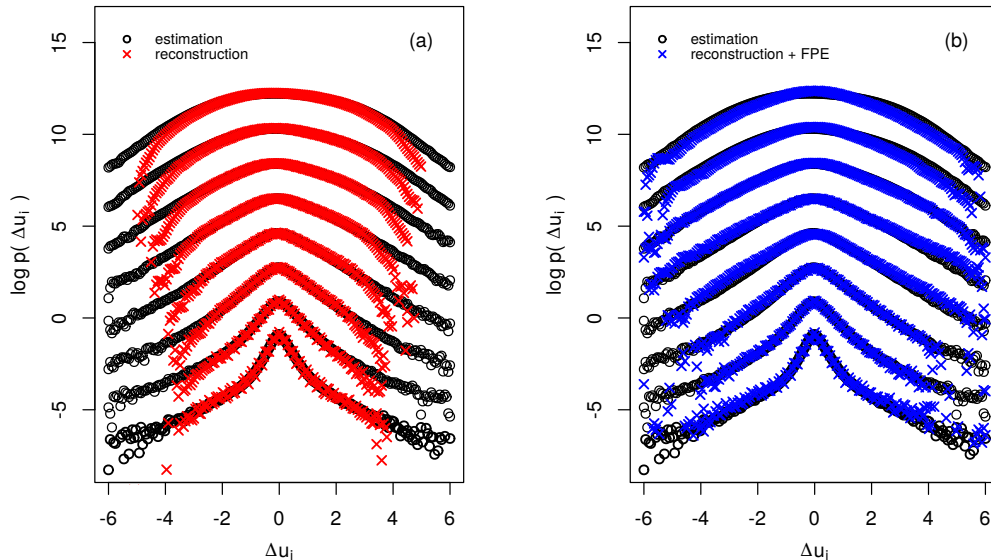


Figure 7. Comparison of the marginal increment pdfs computed from the empirical data (black), the simulated data using the directly estimated pdfs (red) and the simulated data using the [conditional-pdfs-cpdfs](#) obtained from numerical solution of the FPE (blue). The scales range from $\Delta\tau_{ME}$ to $N \cdot \tau_{ME}$, they are explicitly: $2^i \cdot \Delta\tau_{ME}$ with $(i = 0, 1, \dots, 7)$ and $\Delta\tau_{ME} = 0.1$ s. For better visualization the pdfs were shifted along the vertical axis.

$D^{(1)}(u, r, u^*)$ and $D^{(2)}(u, r, u^*)$ is based on observational u data, too (cf. eq. 5). Furthermore the parametrization of these functions is always only a approximation of the real drift and diffusion functions, introducing deviations from the real world system.

But we see from fig. 7) that the majority of increments are well grasped, only the occurrence of a few rare events are under predicted. A more detailed investigation of the pdfs shows the pdfs obtained by the FPE deviates from the original shape for the largest scale $\tau = N \cdot \Delta\tau_{ME}$, but is performing better in the outer wings of the pdf.

From fig. 8 a better understanding of the reconstruction method can be gained: The pdf used for the simulation $p(u^* | u_1, \dots, u_N)$ is not stationary, even though it is computed from completely stationary [conditional-pdfs-cpdfs](#) (cf. 8) and changes sensitively with respect to the N past values. While the snapshot pdf (shown as black circles) at the time marked by the black vertical line has a rather clear shape, it undergoes a change, becoming broader (red line and red circles). Due to the spreading of the wings of the pdf, values of u^* of larger magnitude become more likely to be drawn. This may lead to a distinct shift of the wind speed values to $u^* \leq 0$ as seen in this example. After this transition the broadness decreases (blue line and circles) again and a tendency to relax back to $u^* = 0$ can be seen. Furthermore the increased broadness of the red pdf (red line) can be seen as an early warning signal that the wind speed is prone to fluctuate in a stronger way.

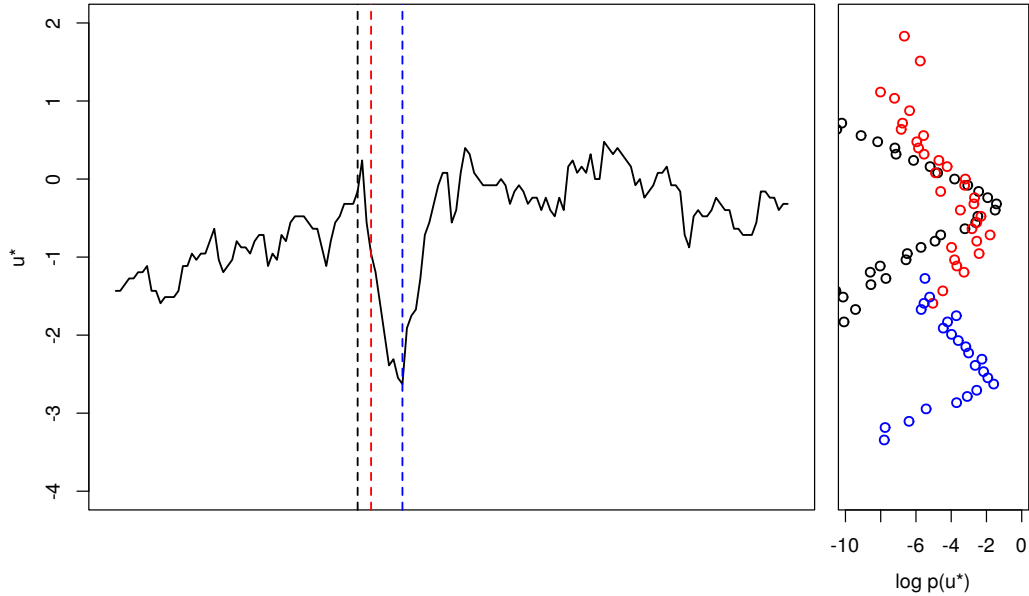


Figure 8. Evolution of $p(u^* | u_1, \dots, u_N)$ during reconstruction. Horizontal lines indicate snapshots of the pdf used for drawing the next sample of u^* . The colors of the horizontal lines respectively correspond to the snapshot pdfs.

3 Extension to non-stationary wind speeds

In the preceding part for the reconstruction scheme block-wise normalized wind speeds with a window length of 1 min were used. These blocks were defined by common mean wind speed \bar{U} and standard deviation σ_U . For the normalised wind speed u we showed how to generate new time series see Fig. 9.

There are different methods to generate more general non-stationary wind data. Knowing the slow variation of $\bar{U}(t)$ and $\sigma_U(t)$ the drift and diffusion coefficients $D^{(i)}$ are taken as slowly changing function of $D^{(i)}(\Delta u, \tau, u^*, \bar{U}, \sigma_U)$. If due to the normalisation of U to u the coefficients $D^{(i)}$ are in a good approximation independent on \bar{U} and σ_U , the slow variation of the real wind conditions can be incorporated over the backtransformation of the newly estimated values $U^* = (\sigma_U \cdot u^*) + \bar{U}$. The slow dynamics of $\bar{U}(t)$ and $\sigma_U(t)$ may be given from measured data, meteorological simulations or other modelling.

A third possibility is a self-adaptive procedure which we show here. Instead of using given values of $\bar{U}(t)$ and $\sigma_U(t)$, the intrinsic fluctuation of these quantities are used: Given an initial pair $(\bar{U}(t), \sigma_U(t))$ estimated over 1 min from measured data, a time series of non-stationary wind-speeds $U^*(t)$ is obtained by applying the above mentioned backtransformation to the generated wind speeds u^* from our algorithm. For the upcoming simulation window of 1 min length a new pair $(\bar{U}(t'), \sigma_U(t'))$

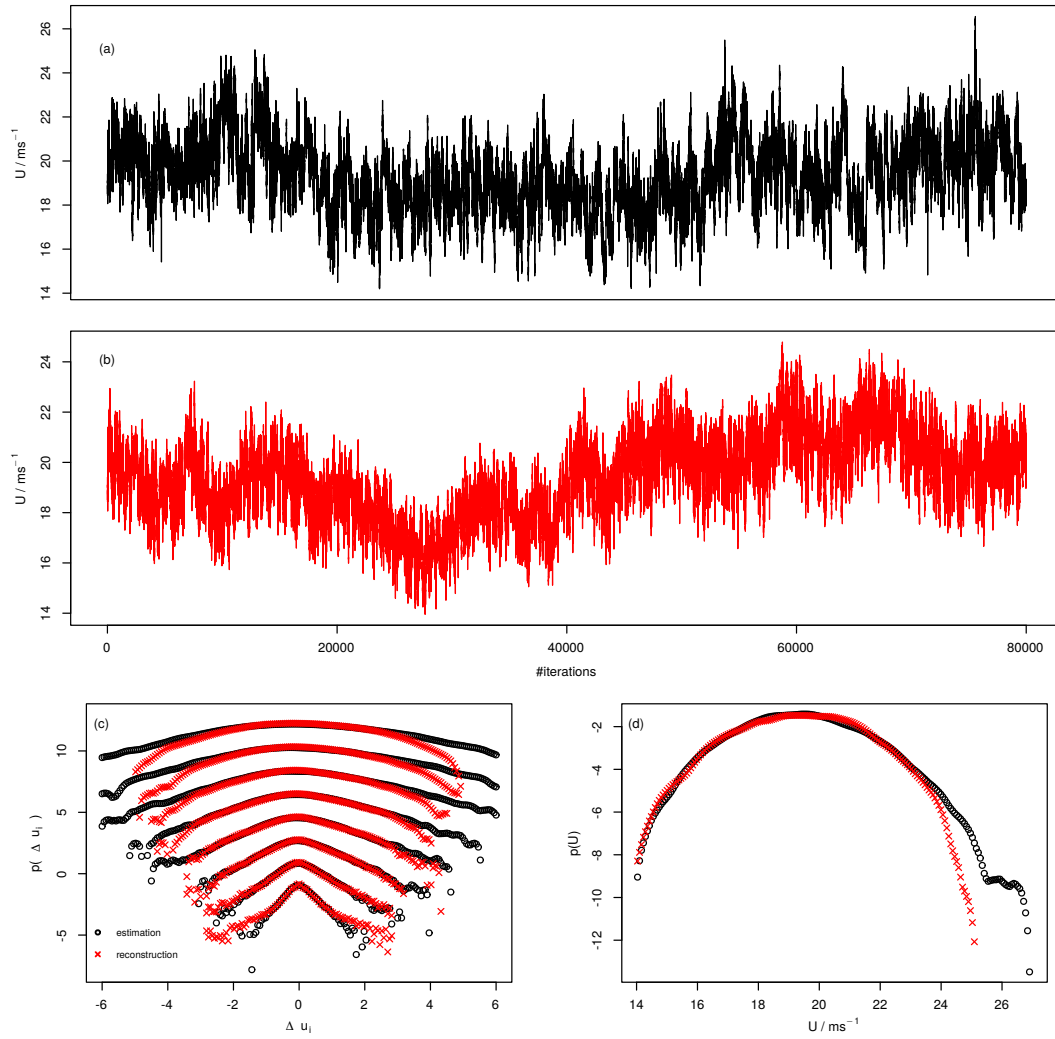


Figure 9. Upper-panel (a), (b): comparison between measured non-stationary speeds U and reconstructed non-stationary wind speeds. Lower panel: increment (left) (c), (d): increment and one point (right) pdfs of original and reconstructed U .

is estimated from the just generated block of wind speed data $U^*(t)$. This procedure is carried out until a time series of non-stationary wind speeds of desired length is obtained. In fig. 9 such a time series is shown together with the statistical analysis of the increment pdfs and the marginal pdf of the non-stationary wind speed U . We observe ~~a fairly nice match between the empirically and reconstructed pdfs~~ that the pdfs of the reconstructed time series match the shape of the empirical pdfs for both, the increments and the wind speeds. At this point we would like to emphasize that we do not aim to create copies of historical wind speeds, but to be able to generate stochastic equivalent time series.

4 Conclusions

We presented a stochastic approach based on multipoint statistics to generate surrogate short time wind speed fluctuations with stochastic processes. Note these stochastic processes can be estimated self-consistently from given data. By using the normalized wind speeds u^* and wind speed increments $\Delta u(\tau_i)$, $\Delta u(\tau_j)$ from two separate scales τ_i and τ_j a three-point closure to the complex systems of wind speeds was achieved.

It was shown that our method works well in describing the dynamics of block-wise normalized wind speeds u^* along scales τ_i in terms of a stochastic scales process, governed by a family of Fokker-Planck equations. This separation of the fluctuations from the mean values is similar to ~~RANS-approach~~ the Reynolds-averaged Navier–Stokes (RANS) approach widely used in fluid dynamics (Frisch, 2004), with the ~~great~~ difference that we have a description of the underlying stochastic process of the fluctuation and 'only' lack the mean values. With the modified reconstruction (cf. sec. 3) we are able to generate mean values on basis of past values of the reconstructed time series, yielding realistic non-stationary wind speed time series U^* . As the typical response times of wind turbines and their control systems have duration of seconds to minutes, our reconstructed wind data are suitable for investigation of many dynamical effects of the wind energy conversion process. Note for these times the wind energy system may be driven in non-stationary response dynamics. Thus for these time scales it is important to have to maximal information on all statistical details of the driving wind source. The stochastic model presented here is based on multipoint statistics and ~~thus captures~~ is able to capture small scale intermittency effects, extreme events as well as clustering of fluctuations, up to not addressed in wind energy research.

For time scales larger than the response times of wind turbines, the turbines operate with fully adapted control systems in a stationary state. To estimate effects, like e.g. loads, of such stationary states the temporal order of the states becomes unimportant. It is sufficient to know how often which wind situation emerges. Thus the knowledge of the valid Weibull distribution $p(\bar{U})$ should be sufficient. Note, our result here indicates that it would be better to extend the Weibull distribution to the joint probability $p(\bar{U}, \sigma_U)$.

Finally we emphasise that the presented stochastic multipoint approach to small scale wind speed fluctuations should encompass automatically extreme short term wind fluctuation, commonly added to investigation in term of standard one or multi-year gusts. This methods can be applied easily to other wind quantities like the temporal behaviour of shears, or wind veers, eventually combined in higher dimensional stochastic processes (Siefert and Peinke, 2006). The results reported in (Ali et al., 2019) show that such a stochastic modelling can also be used for wake flows.

295 **acknowledgement**Acknowledgement: We acknowledge the funding of this project by the VolkswagenStiftung grant and the support from the Ministry for Science and Culture of the German Federal State of Lower Saxony (Grant No. ZN3045, nieders. Vorab to M. W.). Furthermore we acknowledge helpful discussions with AndeAndré Fuchs and Hauke Hähne.

Appendix A: Derivation of simpler cdfs

300 To link equation (2) to the idea of an underlying turbulent cascade we identify the conditional pdf on the left-hand side (lhs) with the cpdf $p(u^*, t^* | \Delta u_1, t^* - \tau_1; \dots; \Delta u_N, t^* - \tau_N)$. Thus the numerator of the right-hand side (rhs of (2) can be rewritten as

$$p(u^*, t^*; u_1, t^* - \tau_1; \dots; u_N, t^* - \tau_N) = \frac{p(u^*, u^* - u_1, \tau_1; \dots; u^* - u_N, \tau_N)}{\dots} \quad (\text{A1})$$

and the nominator as

$$p(u_1, t^* - \tau_1; \dots; u_N, t^* - \tau_N) = \frac{p(u_1; u_1 - u_2, \tau_2 - \tau_1; \dots; u_1 - u_N, \tau_N - \tau_1)}{\dots} \quad (\text{A2})$$

305 The identity of the expressions in (A1) and (A2) can mathematically rigorously be shown, as done in (Nawroth et al., 2010), but intuitively speaking the sequences on the lhs and rhs must yield the same joint pdf, since the increments on the rhs respectively have a common reference point u^* or u_1 . Next we factorize the joint pdfs from equations (A1) and (A2) by iteratively using cpdfs

$$p(u^*; \Delta u_1, \tau_1; \dots; \Delta u_N, \tau_N) = \frac{p(\Delta u_1, \tau_1 | \Delta u_2, \tau_2; \dots; \Delta u_N, \tau_N; u^*) \cdot p(\Delta u_2, \tau_2 | \Delta u_3, \tau_3; \dots; \Delta u_N, \tau_N; u^*) \cdots p(\Delta u_{N-1}, \tau_{N-1} | \Delta u_N, \tau_N; u^*) \cdot p(\Delta u_N, \tau_N | u^*) \cdot p(u^*)}{\dots} \quad (\text{A3})$$

310 and with $\tilde{\Delta} u_i := u(t^* - \tau_1) - u(t^* - \tau_i)$ with the time scale $\tau_i - \tau_1$:

$$p(u_1; \tilde{\Delta} u_2, \tau_2 - \tau_1; \dots; \tilde{\Delta} u_N, \tau_N - \tau_1) = \frac{p(\tilde{\Delta} u_2, \tau_2 - \tau_1 | \tilde{\Delta} u_3, \tau_3 - \tau_1; \dots; \tilde{\Delta} u_N, \tau_N - \tau_1; u_1) \cdot p(\tilde{\Delta} u_3, \tau_3 - \tau_1 | \tilde{\Delta} u_4, \tau_4 - \tau_1; \dots; \tilde{\Delta} u_N, \tau_N - \tau_1; u_1) \cdots p(\tilde{\Delta} u_{N-1}, \tau_{N-1} - \tau_1 | \tilde{\Delta} u_N, \tau_N - \tau_1; u_1) \cdot p(\tilde{\Delta} u_N, \tau_N - \tau_1 | u_1) \cdot p(u_1)}{\dots} \quad (\text{A4})$$

A further step in reducing the dimensionality of the involved pdfs can be performed upon assuming the scale process to be Markovian, i.e. there exists a time scale separation $\Delta\tau_{ME} = \tau_j - \tau_i$ ($j > i$), where

$$p(\Delta u_i, \tau_i | \Delta u_j, \tau_i + \Delta\tau_{ME}; \dots; \Delta u_n, \tau_i + n \cdot \Delta\tau_{ME}; u^*) = p(\Delta u_i, \tau_i | \Delta u_j, \tau_i + \Delta\tau_{ME}; u^*) \quad (\text{A5})$$

315 holds. The time scale separation $\Delta\tau_{ME}$ is often called Markov-Einstein length (Einstein, 1905) and for various systems its existence could be shown empirically, ranging from jet streams in laboratory experiments (Renner et al., 2001), (Reinke et al., 2018) to large geophysical systems such as ocean gravity waves (Hadjihosseini et al., 2016).

Appendix B: Parametrization of $D^{(1)}$ and $D^{(2)}$

320 Here we present the polynomial coefficients used to parametrize the first and second Kramers-Moyal coefficients $D^{(1)}(\Delta u_i, \tau_i, u^*)$ and $D^{(2)}(\Delta u_i, \tau_i, u^*)$ (see eq. 12 and 13).

Coefficients for the drift function $D^{(1)}(\Delta u_i, \tau_i, u^*)$:

$$d_{10} = c_{0,d_{10}} \cdot \tau_i + c_{1,d_{10}} \cdot u^* \cdot \tilde{c}_{1,d_{10}} + c_{2,d_{10}} \cdot \tau_i \cdot \tilde{c}_{2,d_{10}} \cdot u^{*2} + c_{3,d_{10}} \cdot u^{*3} \quad (\text{B1})$$

$$d_{11} = c_{0,d_{11}} \cdot \tau_i + c_{1,d_{11}} \cdot \tau_i \cdot \tilde{c}_{1,d_{11}} + c_{2,d_{11}} \cdot \tau_i \cdot \tilde{c}_{2,d_{11}} \cdot u^{*2} \quad (\text{B2})$$

$$d_{13} = c_{0,d_{13}} \cdot \tau_i \cdot \tilde{c}_{0,d_{13}} + c_{1,d_{13}} \cdot u^* \quad (\text{B3})$$

$$325 \quad \gamma_{D^{(1)}} = c_{1,\gamma_{D^{(1)}}} \cdot \tau_i \cdot \tilde{c}_{1,\gamma_{D^{(1)}}} \cdot u^* \quad (\text{B4})$$

with:

$$c_{0,d_{10}} = -0.006, c_{1,d_{10}} = -0.888, \tilde{c}_{1,d_{10}} = 0.098, c_{2,d_{10}} = 0.137, \tilde{c}_{2,d_{10}} = 0.019, c_{3,d_{10}} = -10.566, c_{0,d_{11}} = -1.656, c_{1,d_{11}} = -0.018, \tilde{c}_{1,d_{11}} = -8.853e - 05, c_{2,d_{11}} = -0.268, \tilde{c}_{2,d_{11}} = 1.671, c_{0,d_{13}} = -0.005, \tilde{c}_{0,d_{13}} = 0.012, c_{1,d_{13}} = 1.023, c_{1,\gamma_{D^{(1)}}} = 0.341, \tilde{c}_{1,\gamma_{D^{(1)}}} = 0.247.$$

330

And for the diffusion function $D^{(2)}(\Delta u_i, \tau_i, u^*)$:

$$d_{20} = c_{0,d_{20}} \cdot \tau_i \cdot \tilde{c}_{0,d_{20}} + c_{1,d_{20}} \cdot \tau_i \cdot \tilde{c}_{1,d_{20}} \cdot u^* + c_{2,d_{20}} \cdot \tau_i \cdot \tilde{c}_{2,d_{20}} \cdot u^{*2} \quad (\text{B5})$$

$$d_{21} = c_{0,d_{21}} \cdot \tau_i \cdot \tilde{c}_{0,d_{21}} + c_{1,d_{21}} \cdot \tau_i \cdot \tilde{c}_{1,d_{21}} \cdot u^* \quad (\text{B6})$$

$$d_{22} = c_{0,d_{22}} \cdot \tilde{\tau}_i^{\tilde{c}_{0,d_{22}}} + c_{1,d_{22}} \cdot \tilde{\tau}_i^{\tilde{c}_{1,d_{22}}} \cdot u^* \quad (\text{B7})$$

335 with:

$$\begin{aligned} c_{0,d_{20}} = 0.024, \tilde{c}_{0,d_{20}} = -0.0001, c_{1,d_{20}} = 0.0002, \tilde{c}_{1,d_{20}} = 1.076, c_{2,d_{20}} = 1.573, \tilde{c}_{2,d_{20}} = 1.622, c_{0,d_{21}} = 0.002, \tilde{c}_{0,d_{21}} = -0.001, \\ c_{1,d_{21}} = 1.104, \tilde{c}_{1,d_{21}} = 1.395, c_{0,d_{22}} = 0.042, \tilde{c}_{0,d_{22}} = 0.002, c_{1,d_{22}} = 0.555, \tilde{c}_{1,d_{22}} = 0.364. \end{aligned}$$

References

- IEC 61400-1 Wind turbines Part 1: Design requirements, 2005.
- 340 Ali, N., Fuchs, A., Neunaber, I., Peinke, J., and Cal, R. B.: Multi-scale/fractal processes in the wake of a wind turbine array boundary layer, *J TURBUL*, 20, 93–120, <https://doi.org/10.1080/14685248.2019.1590584>, 2019.
- Anvari, M., Lohmann, G., Wächter, M., Milan, P., Lorenz, E., Heinemann, D., Tabar, M. R. R., and Peinke, J.: Short term fluctuations of wind and solar power systems, *New J. Phys.*, 18, 063 027, <https://doi.org/10.1088/1367-2630/18/6/063027>, 2016.
- Boettcher, F., Renner, C., Waldl, H.-P., and Peinke, J.: On the statistics of wind gusts, *Boundary-Layer Meteorology*, 108, 163–173, 345 <https://doi.org/10.1023/A:1023009722736>, 2003.
- Carpinone, A., Langella, R., Testa, A., and Giorgio, M.: Very short-term probabilistic wind power forecasting based on Markov chain models, 2010 IEEE 11th International Conference on Probabilistic Methods Applied to Power Systems, 2010.
- Einstein, A.: Über die von der molekularkinetischen Theorie der Wärme geforderte Bewegung von in ruhenden Flüssigkeiten suspendierten Teilchen, *Ann. Phys.*, 322, 549–560, <https://doi.org/10.1002/andp.19053220806>, 1905.
- 350 Friedrich, R., Peinke, J., Sahimi, M., and Tabar, M. R. R.: Approaching complexity by stochastic methods: From biological systems to turbulence, *Phys. Rep.*, 506, 87 – 162, <https://doi.org/10.1016/j.physrep.2011.05.003>, 2011.
- Frisch, U.: *Turbulence: The Legacy of A. N. Kolmogorov*, vol. 1, Cambridge Univ. Press, 2004.
- Hadjihoseini, A., Lind, P. G., Mori, N., Hoffmann, N. P., and Peinke, J.: Rogue waves and entropy consumption, *EPL*, 120, 30 008, <https://doi.org/10.1209/0295-5075/120/30008>, 2018.
- 355 Hadjihosseini, A., Wächter, M., P.Hoffmann, N., and Peinke, J.: Capturing rogue waves by multi-point statistics, *New J. Phys.*, 18, 013 017, <https://doi.org/10.1088/1367-2630/18/1/013017>, 2016.
- Haehne, H., Schottler, J., Waechter, M., Peinke, J., and Kamps, O.: The footprint of atmospheric turbulence in power grid frequency measurements, *EPL*, 121, 30 001, <https://doi.org/10.1209/0295-5075/121/30001>, 2018.
- K, B. and L, K. J.: Pitfalls of modeling wind power using Markov chains, 2009 IEEE/PES Power Systems Conference and Exposition, pp. 360 1–6, 2009.
- Milan, P., Wächter, M., and Peinke, J.: Turbulent Character of Wind Energy, *Phys. Rev. Lett.*, 110, 138 701, <https://doi.org/10.1103/PhysRevLett.110.138701>, 2013.
- Morales, A., Waechter, M., and Peinke, J.: Characterization of wind turbulence by higher-order statistics, *Wind Energy*, 15, 391–406, <https://doi.org/10.1002/we.478>, 2012.
- 365 Mücke, T., Kleinhans, D., and Peinke, J.: Atmospheric turbulence and its influence on the alternating loads on wind turbines, *Wind Energy*, 14, 301–316, <https://doi.org/10.1002/we.422>, 2011.
- Nawroth, A. P. and Peinke, J.: Multiscale reconstruction of time series, *Phys. Lett. A*, 360, 234–237, <https://doi.org/10.1016/j.physleta.2006.08.024>, 2006.
- Nawroth, A. P., Friedrich, R., and Peinke, J.: Multi-scale description and prediction of financial time series, *New J. Phys.*, 12, 083 021, 370 <https://doi.org/10.1088/1367-2630/12/8/083021>, 2010.
- Papaefthymiou, G. and Klockl, B.: MCMC for Wind Power Simulation, 2008 IEEE Transactions on Energy Conversion, pp. 234–240, 2008.
- Peinke, J., Tabar, M. R., and Wächter, M.: The Fokker–Planck Approach to Complex Spatiotemporal Disordered Systems, *Annual Review of Condensed Matter Physics*, 10, 107–132, <https://doi.org/10.1146/annurev-conmatphys-033117-054252>, 2019.

- Pesch, T., Schröders, S., Allelein, H. J., and Hake, J. F.: A new Markov-chain-related statistical approach for modelling synthetic wind power time series, *New J. Phys.*, 17, 055 001, <https://doi.org/10.1088/1367-2630/17/5/055001>, 2015.
- 375 Reinke, N., Fuchs, A., Nickelsen, D., and Peinke, J.: On universal features of the turbulent cascade in terms of non-equilibrium thermodynamics, *J. Fluid Mech.*, 848, 117–153, <https://doi.org/10.1017/jfm.2018.360>, 2018.
- Renner, C., Friedrich, R., and Peinke, J.: Experimental indications for Markov properties of small-scale turbulence, *J. Fluid Mech.*, 433, 383–409, <https://doi.org/10.1017/S0022112001003597>, 2001.
- 380 Risken, H.: *The Fokker-Planck-Equation: Methods of Solution and Application*, vol. 2 of *Springer series in synergetics, Berlin*, Springer, 1996.
- Siefert, M. and Peinke, J.: Joint multi-scale statistics of longitudinal and transversal increments in small-scale wake turbulence, *J TURBUL.*, 7, N50, <https://doi.org/10.1080/14685240600677673a>, 2006.
- Stresing, R. and Peinke, J.: Towards a stochastic multi-point description of turbulence, *New J. Phys.*, 12, 103 046, <https://doi.org/10.1088/1367-2630/12/10/103046>, 2010.
- 385 Wächter, M., Riess, F., Kantz, H., and Peinke, J.: Stochastic analysis of surface roughness, *EPL*, 64, 579–585, <https://doi.org/10.1209/epl/i2003-00616-4>, 2003.
- Wächter, M., Milan, P., Mücke, T., and Peinke, J.: Power performance of wind energy converters characterized as stochastic process: applications of the Langevin power curve, *Wind Energy*, 14, 711–717, <https://doi.org/10.1002/we.453>, 2011.
- 390 Weber, J., Zachow, C., and Witthaut, D.: Modeling long correlation times using additive binary Markov chains: Applications to wind generation time series, *Phys. Rev. E*, 97, 032 138, <https://doi.org/10.1103/PhysRevE.97.032138>, 2018.
- WindEurope: *Wind in power 2017*, <https://windeurope.org/wp-content/uploads/files/about-wind/statistics/WindEurope-Annual-Statistics-2017.pdf>, 2018.